Parton Distribution Functions and their applications

Pavel Nadolsky

Department of Physics
Southern Methodist University (Dallas, TX)

Lecture 2
June 20, 2018

Recap, lecture 1

In the first lecture, we discussed the basic behavior of parton distribution functions, motivation for precision studies of PDFs, and key experiments from which the PDFs are determined

Today we will review practical issues associated with the determination and usage of PDFs: differences between the PDF sets, computation of PDF uncertainties, implementation of correlated errors, and combination of PDF sets.

Global QCD analysis

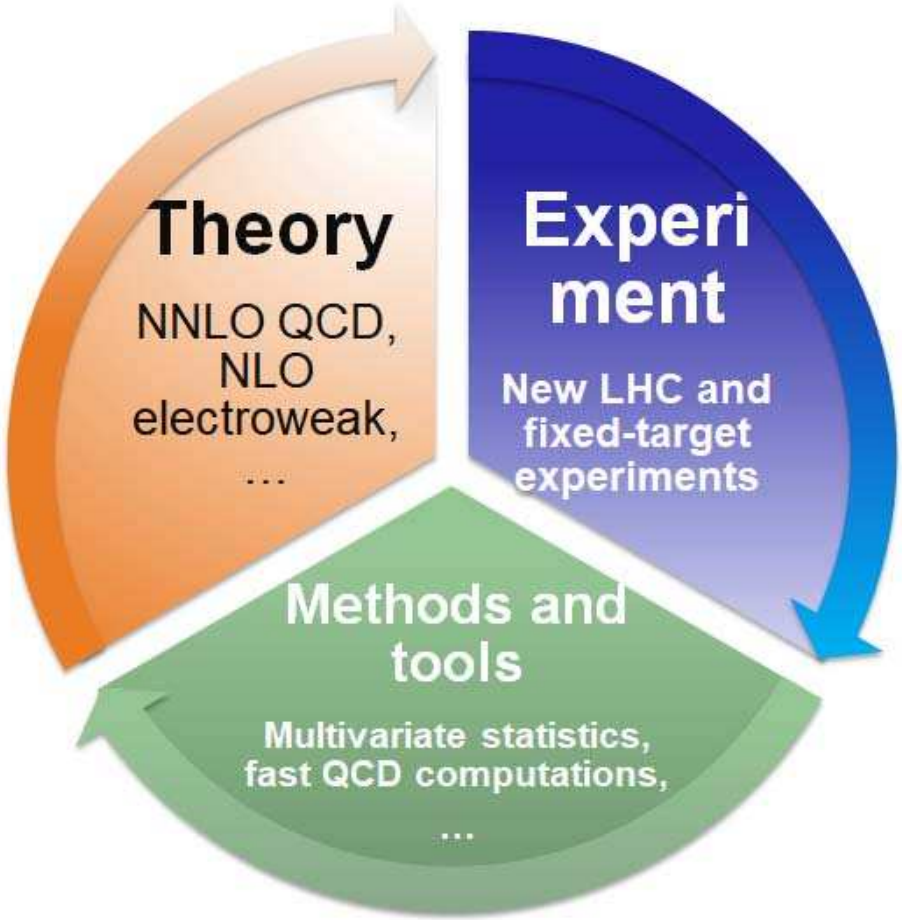

The **global QCD analysis** reveals elaborate connections between advanced **QCD theory**, precise **HEP experiments**, and powerful **statistical methods**

Classes of PDFs

General-purpose

For (N)NLO calculations with
$N_f \leq 5$ active quark flavors

From several groups:
ABMP'16
HERA2.0
CT14 (→ 17p)
MMHT'14 (→ 16)
NNPDF3.0 (→3.1)
…

Specialized

For instance, for CT14:
CT14 LO
CT14 $N_f = 3, 4, 6$
CT14 HERA2
CT14 Intrinsic charm
CT14 QCD+QED
CT14 MC

ATLAS & CMS exploratory

Combined

PDF4LHC'15=CT14+MMHT'14+NNPDF3.0

General-purpose CT14 PDFs

(S. Dulat et al., arXiv:1506.07443)

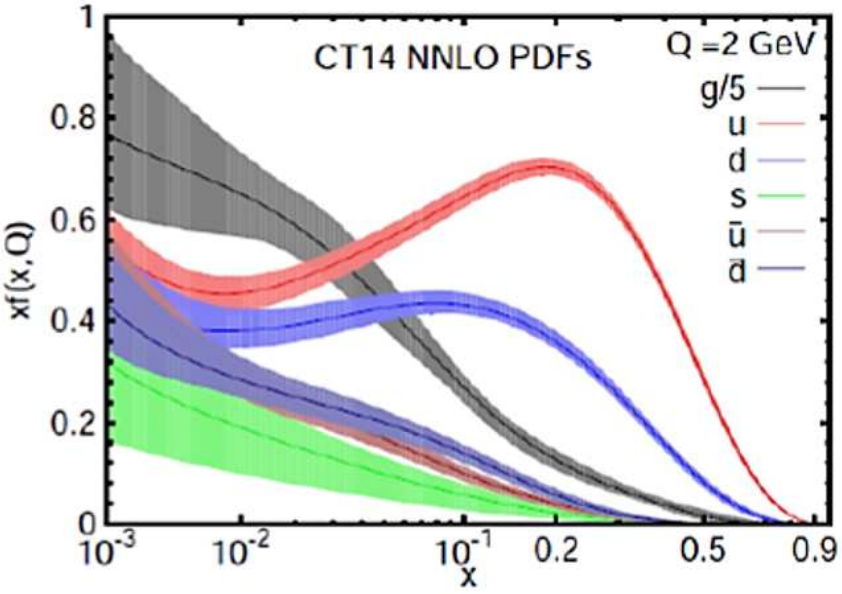

Q= 2 GeV

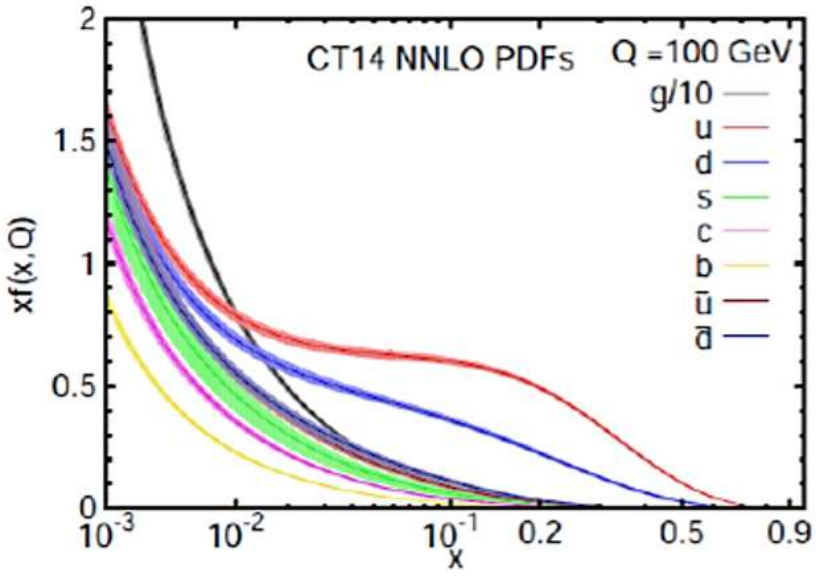

Q= 100 GeV

Phenomenological parametrizations of PDFs are provided with estimated uncertainties of multiple origins (**uncertainties of measurement, theoretical model, parametrization form, statistical analysis**, …)

The shape of PDFs is optimized w.r.t. hundreds of **nuisance parameters**

CT14, MMHT14, NNPDF3.1 PDFs

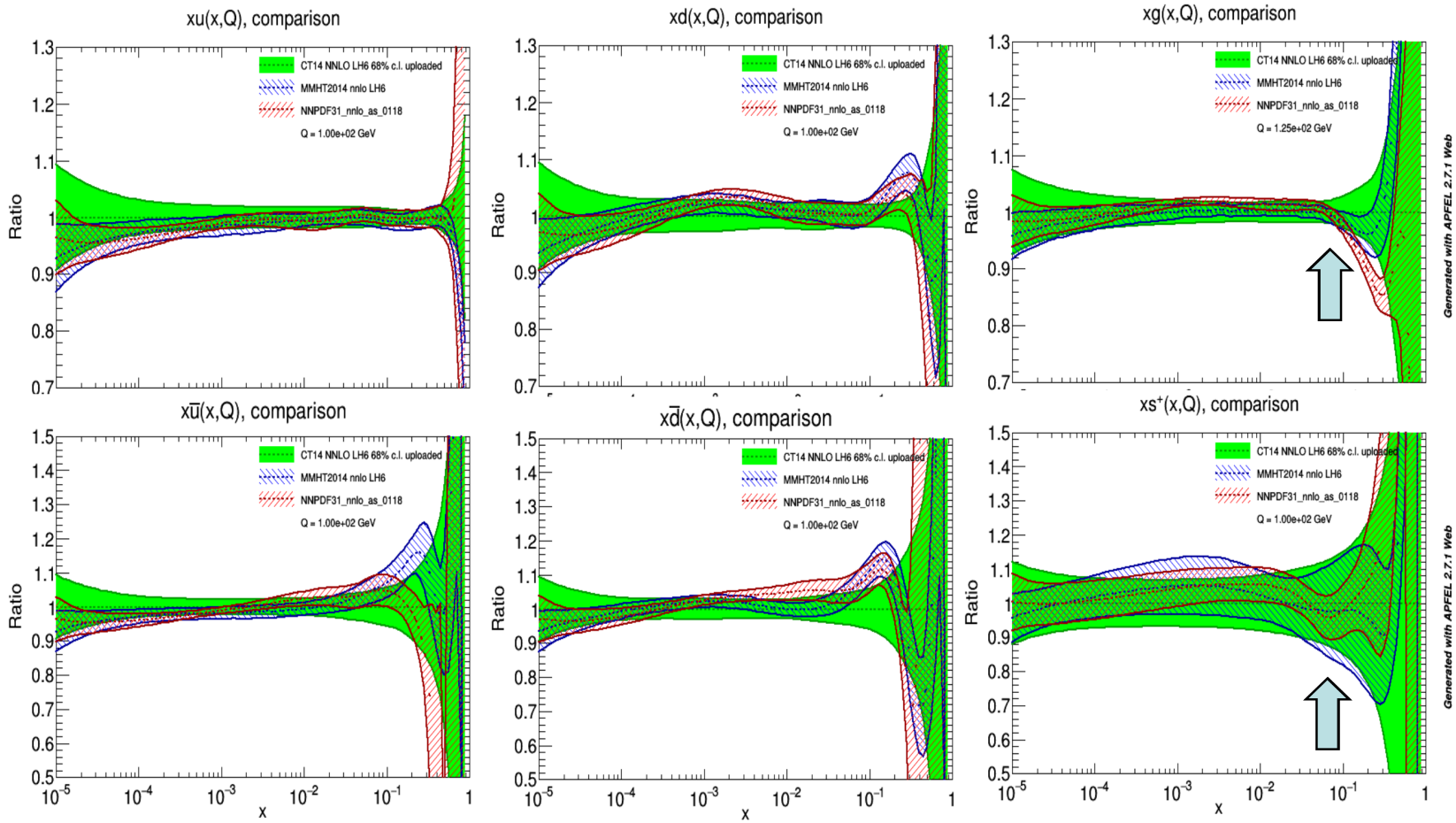

Central PDFs of 3 sets are compatible. The NNPDF3.1 uncertainty is moderately reduced on $g(x,Q)$ at $x > 0.05$, $s + \bar{s}$ at all x. The effect of the LHC data on the error bands does not exceed dependence on the definition of the PDF uncertainty (CT vs. MMHT vs. NNPDF).

HERAPDF2.0 vs. CT14, MMHT14, NNPDF3.0

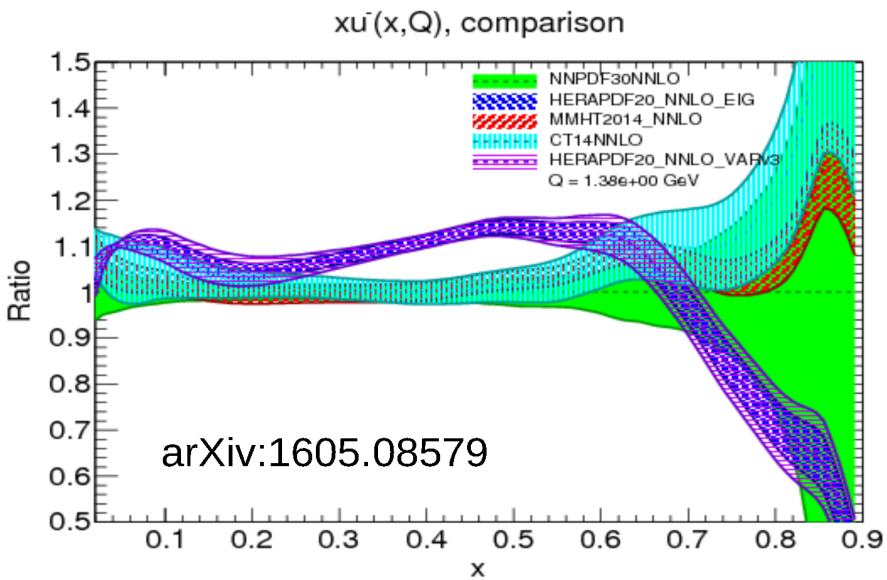

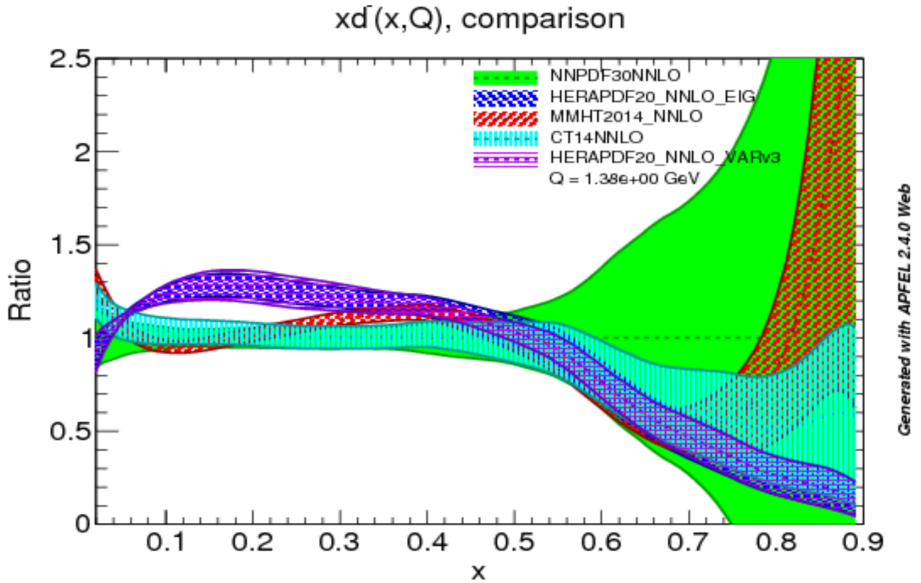

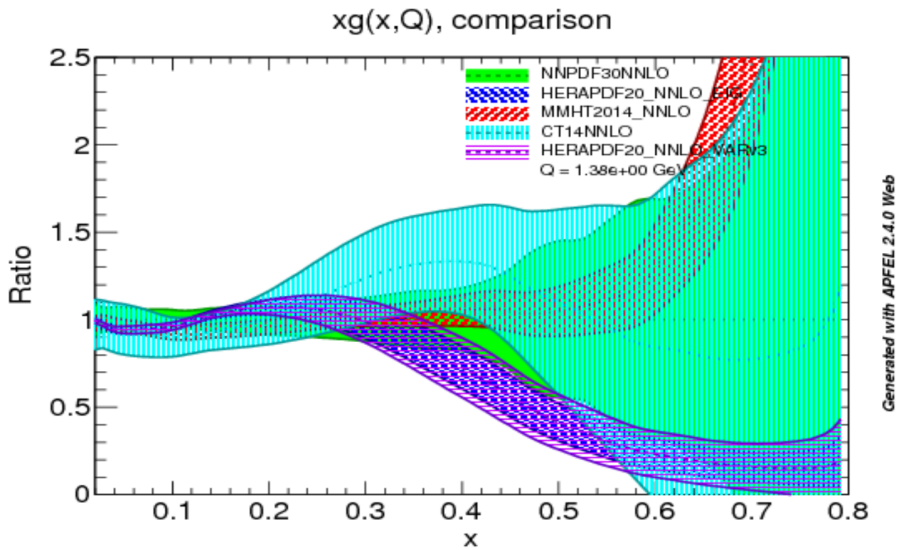

HERAPDF2.0 stands out in the comparison because of its x dependence and smaller PDF uncertainty

Origin of differences between PDF sets

1. Corrections of wrong or outdated assumptions

lead to significant differences between new (≈post-2014) and old (≈pre-2014) PDF sets

- inclusion of NNLO QCD, heavy-quark hard scattering contributions
- relaxation of ad hoc constraints on PDF parametrizations
- improved numerical approximations

Origin of differences between PDF sets

2. PDF uncertainty

a range of allowed PDF shapes for plausible input assumptions, **partly** reflected by the PDF error band

is associated with

- the choice of fitted experiments
- experimental errors propagated into PDF's
- handling of inconsistencies between experiments
- choice of $\alpha_s(M_Z)$,m_c,$m_{b,}$, factorization scales, parametrizations for PDF's, higher-twist terms, nuclear effects,...

leads to non-negligible differences between the newest PDF sets

Stages of the PDF analysis

1. Select valid experimental data
2. Assemble most precise theoretical cross sections and verify their mutual consistency
3. Choose the functional form for PDF parametrizations
4. Implement a procedure to handle nuisance parameters (>200 sources of correlated experimental errors)
5. Perform a fit
6. Make the new PDFs and their uncertainties available to end users

1. Selection of experimental data

- **Neutral-current ep DIS data from HERA are STILL the most extensive and precise** among all data sets
  - In addition, their systematic errors were reduced recently by cross calibration of H1 and ZEUS detectors
- However, by their nature they constrain only a limited number of PDF parameters
- Thus, two complementary approaches to the selection of the data are possible

Two strategies for selection of experimental data

Global analyses *(~ABMP'16, CT14, MMHT'14, NNPDF3.1)* $\Rightarrow$ focus on completeness, reliable flavor decomposition

- all HERA data + fixed-target DIS data
  - notably, CCFR and NuTeV νN DIS constraining $s(x, Q)$
- low-Q Drell-Yan (E605, E866), W lepton asymmetry, Z rapidity and p_T
- Tevatron Run-2 and LHC jet production, $t\bar{t}$ production, $W + c$ production

Restricted analyses $\Rightarrow$ focus on the most precise data, esp. HERA DIS

- NC DIS, CC DIS, NC DIS jet, c and b production *(HERAPDF1.0,1.5, 2,0; ATLAS; CMS; JR)*

Selection of experiments: CT14 NNLO

$Q^2 > 4\ GeV^2$, $W^2 > 12.25\ \ GeV^2$

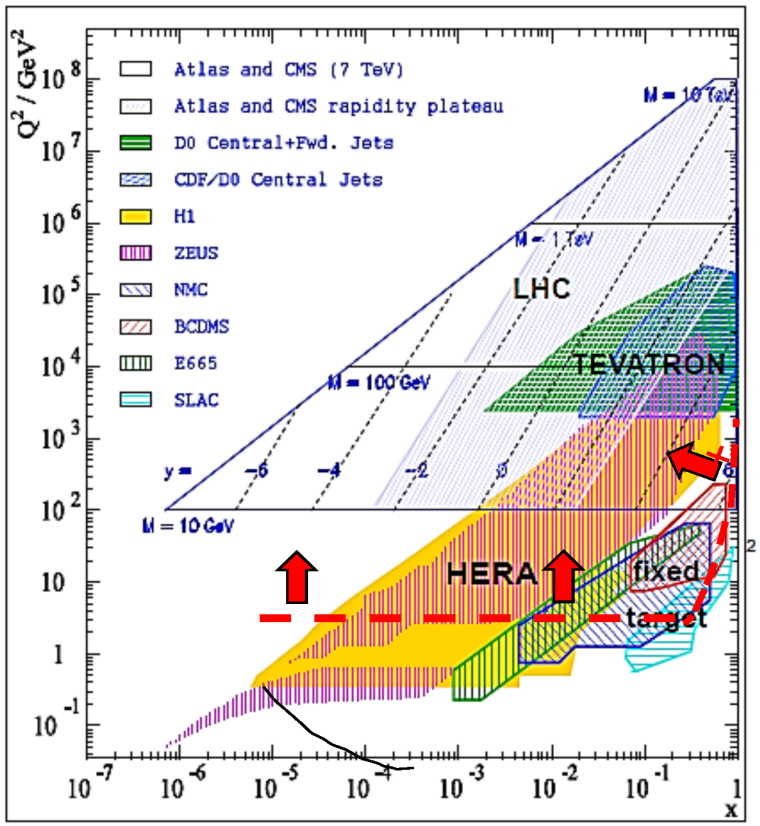

CT14:

only DIS data with above the red line are accepted to ensure stable perturbative predictions

Selection of experiments: CJ15 NLO

$$Q^2 > 1.3\ GeV^2\ ,\ W^2 > 3\ GeV^2$$

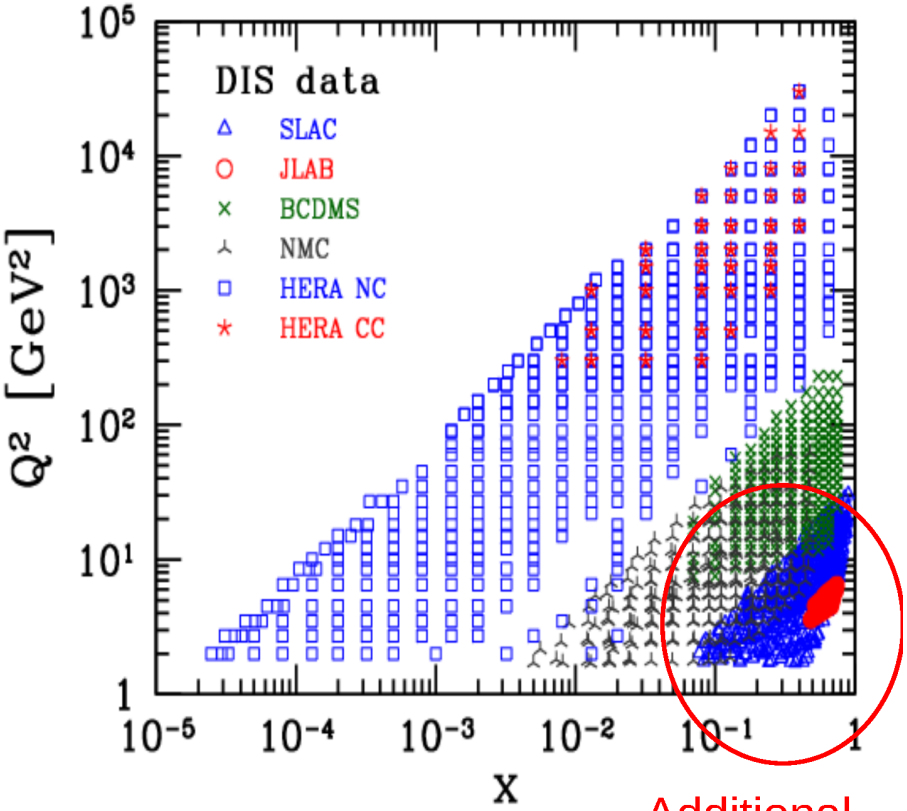

Additional constraints on d/u

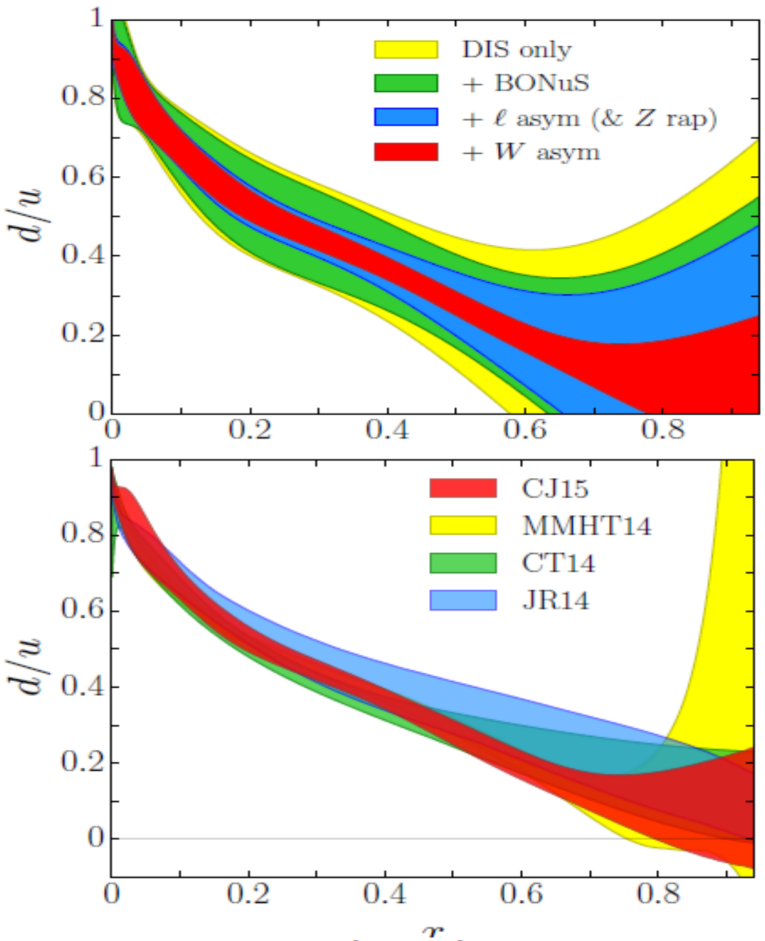

FIG. 16: Comparison of the d/u ratio at $Q^2 = 10$ GeV^2 for different PDF parametrizations: CJ15 (red band), MMHT14 [6] (yellow band), CT14 [7] (green band), and JR14 [10] (blue band).

With CJ selection cuts, higher-twist and nuclear corrections must be applied to DIS cross sections

Ratio $R_s \equiv \frac{(s+\bar{s})}{(\bar{u}+\bar{d})}(x, Q)$

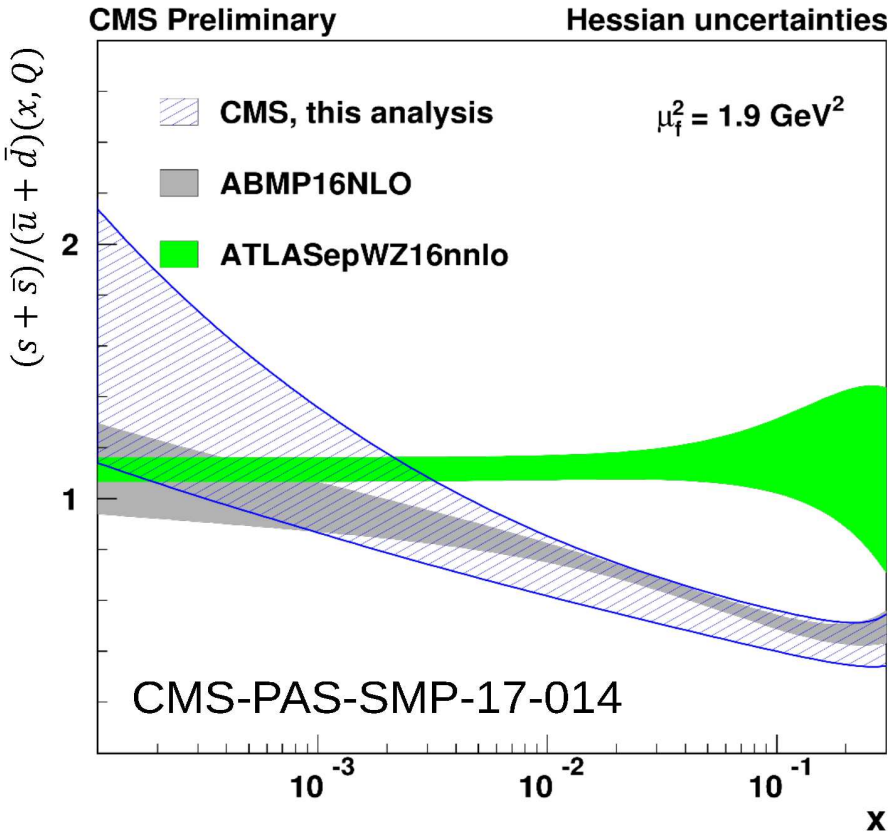

ATLAS and CMS **restricted** analyses of $W, Z, W + c$ production produce uncertainty bands in some tension with one another

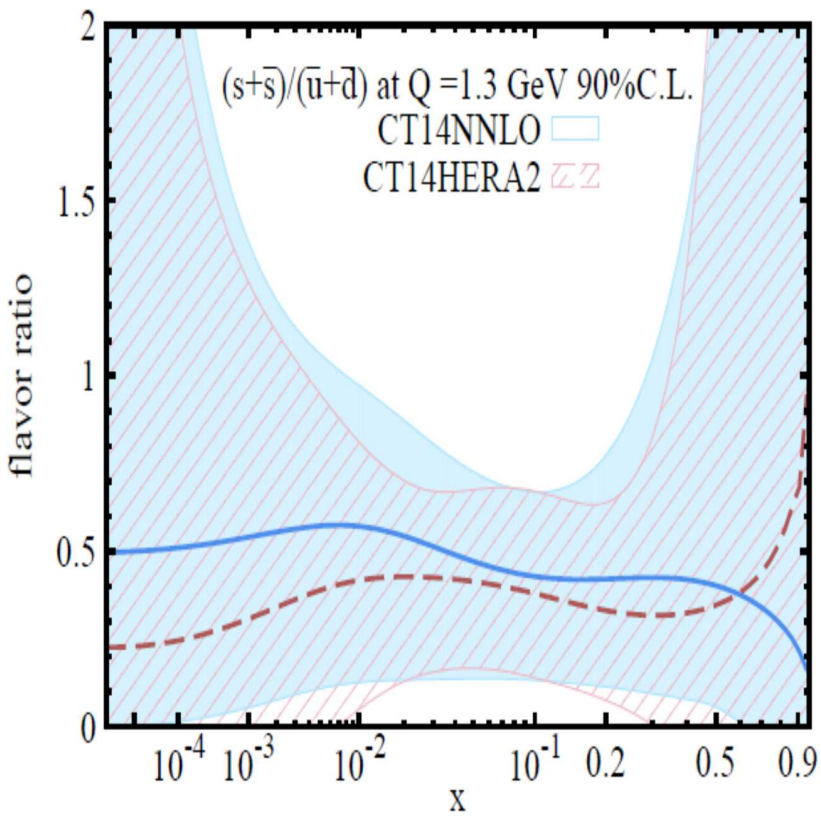

The CT14(HERA2) NNLO **global** analysis predicts a wider uncertainty band that is compatible with ATLAS and CMS solutions

2. Available theoretical cross sections

Process	Number of QCD loops	Mass scheme*	
Neutral current	2	ZM	*Moch, Vermaseren, Vogt*
DIS	2	GM	*Riemersma, Harris, Smith, van Neerven*
			Buza, Matiounine, Smith, van Neerven
Charged current	2	ZM	*Moch, Vermaseren, Vogt*
DIS	2	GM	*Berger et al.*
$pN \xrightarrow{\gamma^*,W,Z} \ell\ell^{(\prime)}X$	2,3	ZM	*Anastasiou et al.; Boughezal et al; Gehrmann*
$p\bar{p} \to jX$	2	ZM	*Gehrmann et al.*
$ep \to jjX$	2	ZM	
$pp \to t\bar{t}X$	2	ZM	*Csakon, Mitov et al.*

*ZM/GM: zero-mass/general-mass approximation for c, b contributions

Breath-taking progress in (N)NNLO calculations!

3. Requirements for PDF parametrizations

A. A valid set of $f_{a/p}(x,Q)$ must satisfy QCD sum rules

Valence sum rule

$$\int_0^1 [u(x,Q)-\bar{u}(x,Q)]\,dx = 2 \qquad \int_0^1 \left[d(x,Q)-\bar{d}(x,Q)\right]\,dx = 1$$

$$\int_0^1 [s(x,Q)-\bar{s}(x,Q)]\,dx = 0$$

A proton has net quantum numbers of 2 u quarks + 1 d quark

Momentum sum rule

$$[\text{proton}] \equiv \sum_{a=g,q,\bar{q}} \int_0^1 x\, f_{a/p}(x,Q)\,dx = 1$$

momenta of all partons must add up to the proton's momentum

Through this rule, normalization of $g(x,Q)$ is tied to the first moments of quark PDFs

3. Requirements for PDF parametrizations

B. A valid PDF set must **not** produce unphysical predictions for observable quantities

Example

- Any concievable hadronic cross section σ must be non-negative: $\sigma \geq 0$
  - this is typically realized by requiring $f_{a/p}(x, Q) > 0$
- Any cross section asymmetry A must lie in the range $-1 \leq A \leq 1$
  - this constrains the range of allowed PDF pararametrizations
- Independent parametrizations for $s - \bar{s}$,γ, c may be difficult to constrain or separate from other factors

PDFs with photons and intrinsic charm

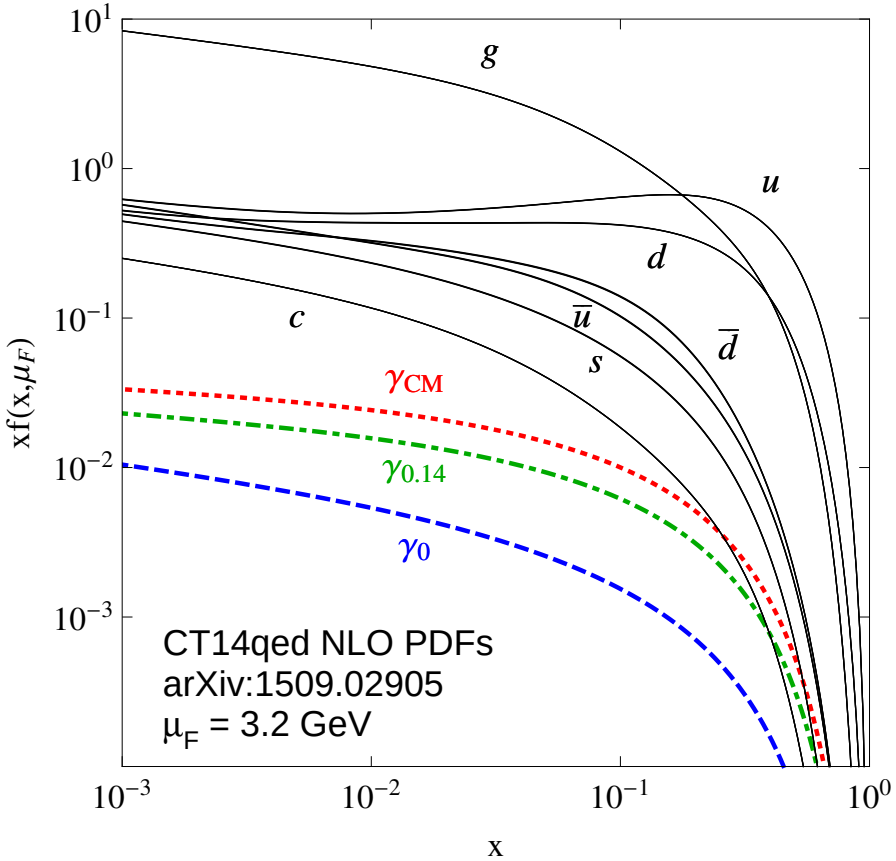

The photon PDF $f_{\gamma/p}(x, Q)$ compared to other flavors

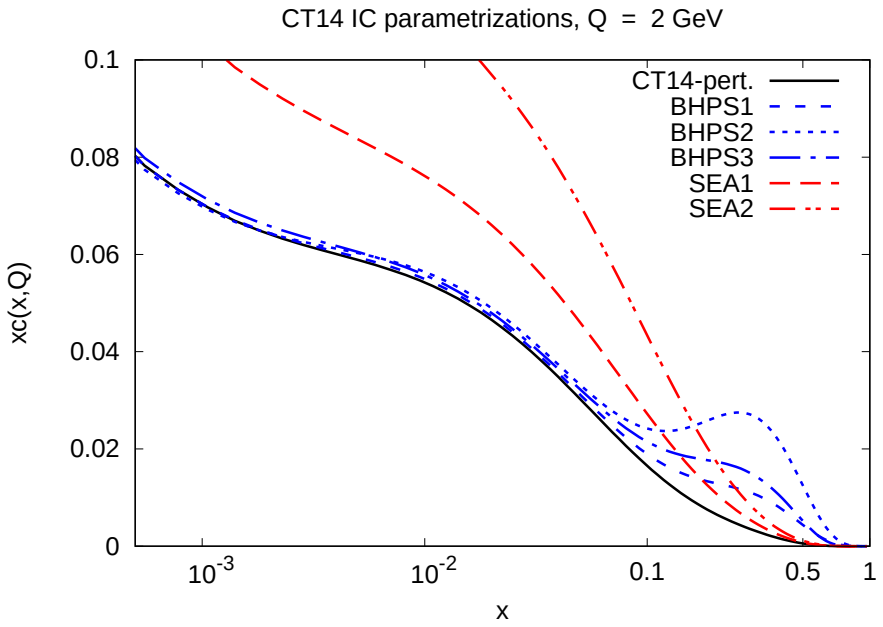

Light-cone model (BHPS) and sea-like (SEA) parametrizations for the "intrinsic charm" PDF *(Hou et al., 1707.00657)*

Requirements for PDF parametrizations

PDF parametrizations for $f_{a/p}(x, Q)$ must be "flexible just enough" to reach agreement with the data, without violating QCD constraints (sum rules, positivity, ...) or reproducing random fluctuations

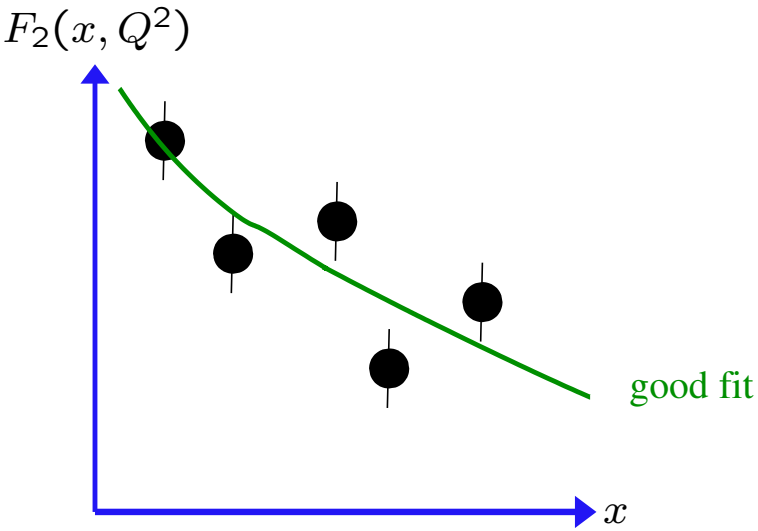

Requirements for PDF parametrizations

PDF parametrizations for $f_{a/p}(x, Q)$ must be "flexible just enough" to reach agreement with the data, without violating QCD constraints (sum rules, positivity, ...) or reproducing random fluctuations

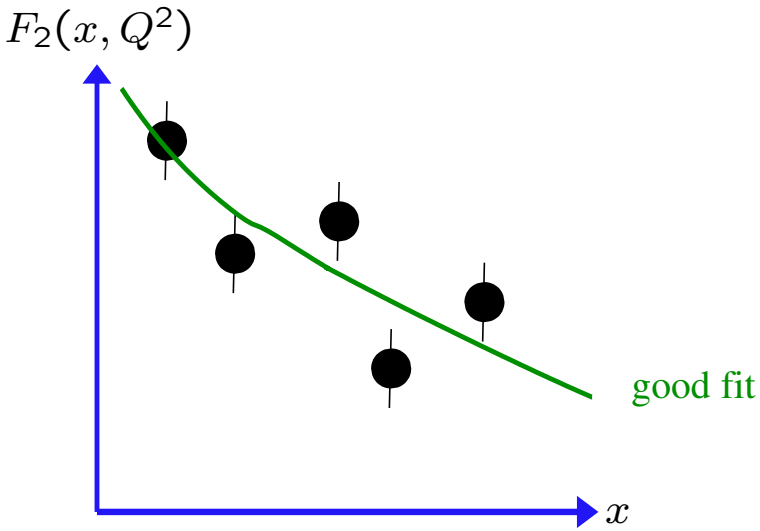

Traditional solution

"Theoretically motivated" functions with a few parameters

$$f_{i/p}(x, Q_0) = a_0 x^{a_1} (1-x)^{a_2} \times F(x;\, a_3, a_4, ...)$$

- $x \to 0$: $f \propto x^{a_1}$ – Regge-like behavior
- $x \to 1$: $f \propto (1-x)^{a_2}$ – quark counting rules

Requirements for PDF parametrizations

PDF parametrizations for $f_{a/p}(x, Q)$ must be "flexible just enough" to reach agreement with the data, without violating QCD constraints (sum rules, positivity, ...) or reproducing random fluctuations

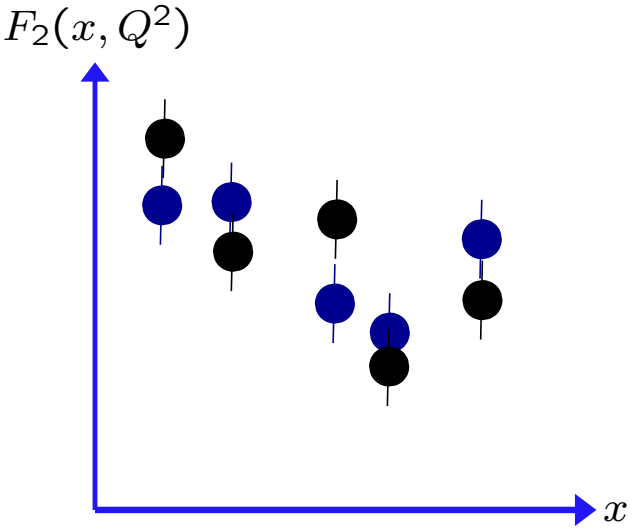

Resampling and bootstrapping

Neural Network PDF collaboration

- Generate N replicas of the experimental data, randomly scattered around the original data in accordance with the probability suggested by the experimental errors
- Divide the replicas into a fitting sample and control sample

Requirements for PDF parametrizations

PDF parametrizations for $f_{a/p}(x, Q)$ must be "flexible just enough" to reach agreement with the data, without violating QCD constraints (sum rules, positivity, ...) or reproducing random fluctuations

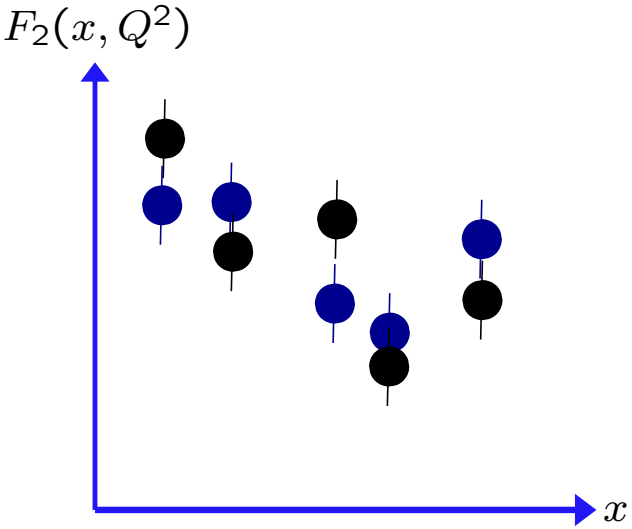

Resampling and bootstrapping

Neural Network PDF collaboration

- Parametrize $f_{a/p}(x, Q)$ by ultra-flexible functions — neural networks
- A statistical theorem states that any function can be approximated by a neural network with a sufficient number of nodes (in practice, of order 10)

Requirements for PDF parametrizations

PDF parametrizations for $f_{a/p}(x, Q)$ must be "flexible just enough" to reach agreement with the data, without violating QCD constraints (sum rules, positivity, ...) or reproducing random fluctuations

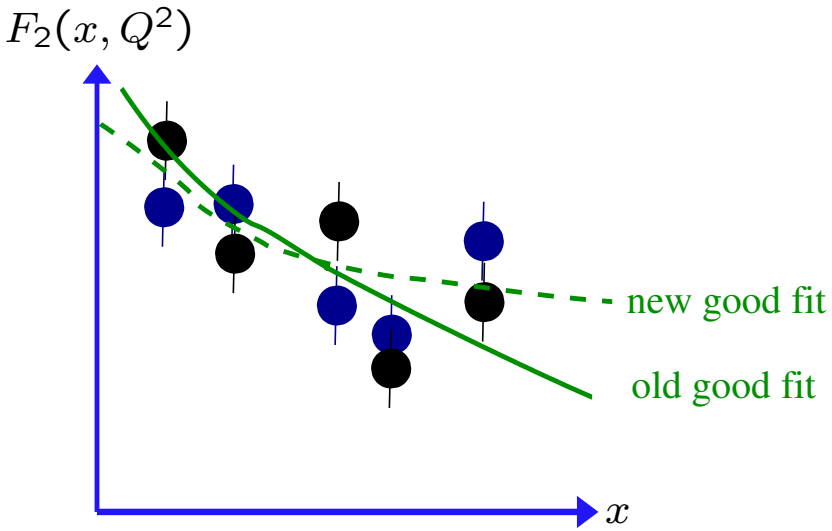

Resampling and bootstrapping

Neural Network PDF collaboration

- Fit the neural nets to the fitting sample, while demanding good agreement with the control sample
- Smoothness of $f_{a/p}(x, Q)$ is preserved, despite its nominal flexibility

Analytic PDF parametrizations (CT10)

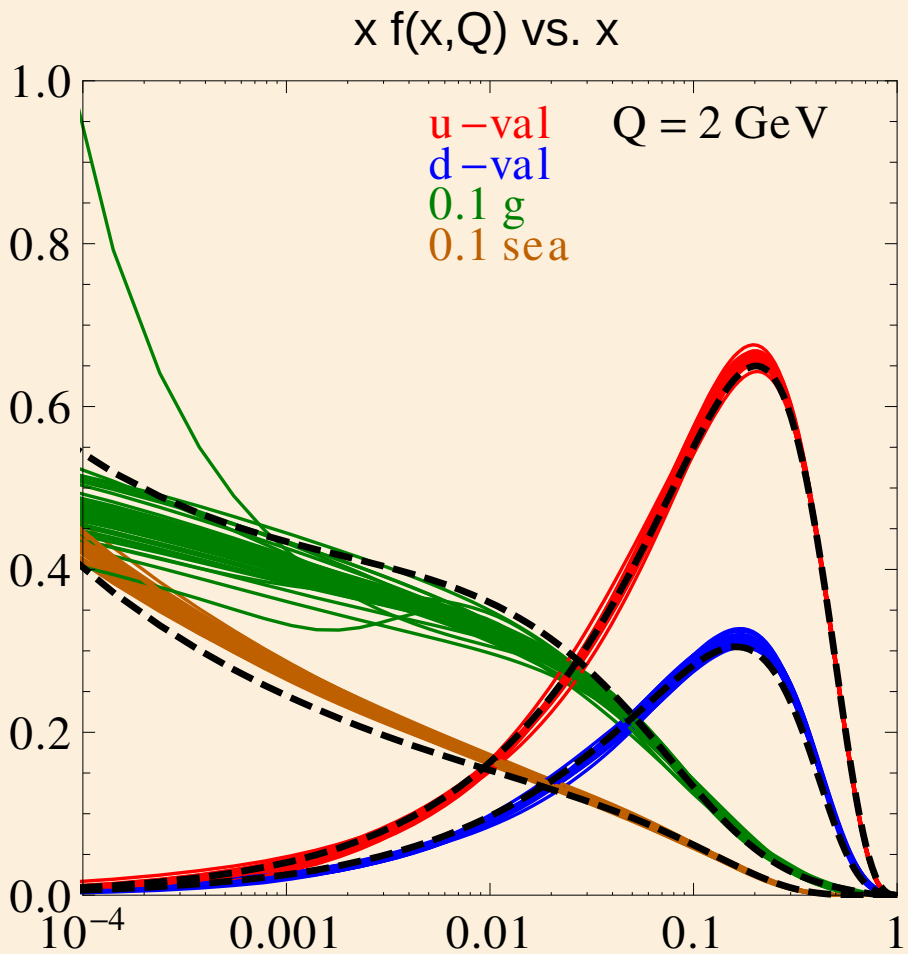

Neural network parametrizations

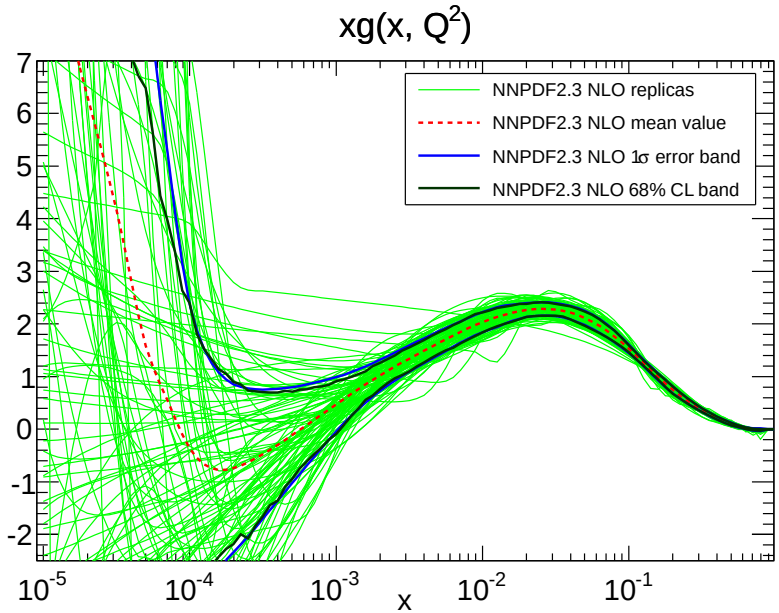

4. Statistical aspects

J. Pumplin et al., JHEP 0207, 012 (2002), and references therein; J. Collins & J. Pumplin, hep-ph/0105207

Who recognizes the formula on the whiteboard?

4. Statistical aspects

J. Pumplin et al., JHEP 0207, 012 (2002), and references therein; J. Collins & J. Pumplin, hep-ph/0105207

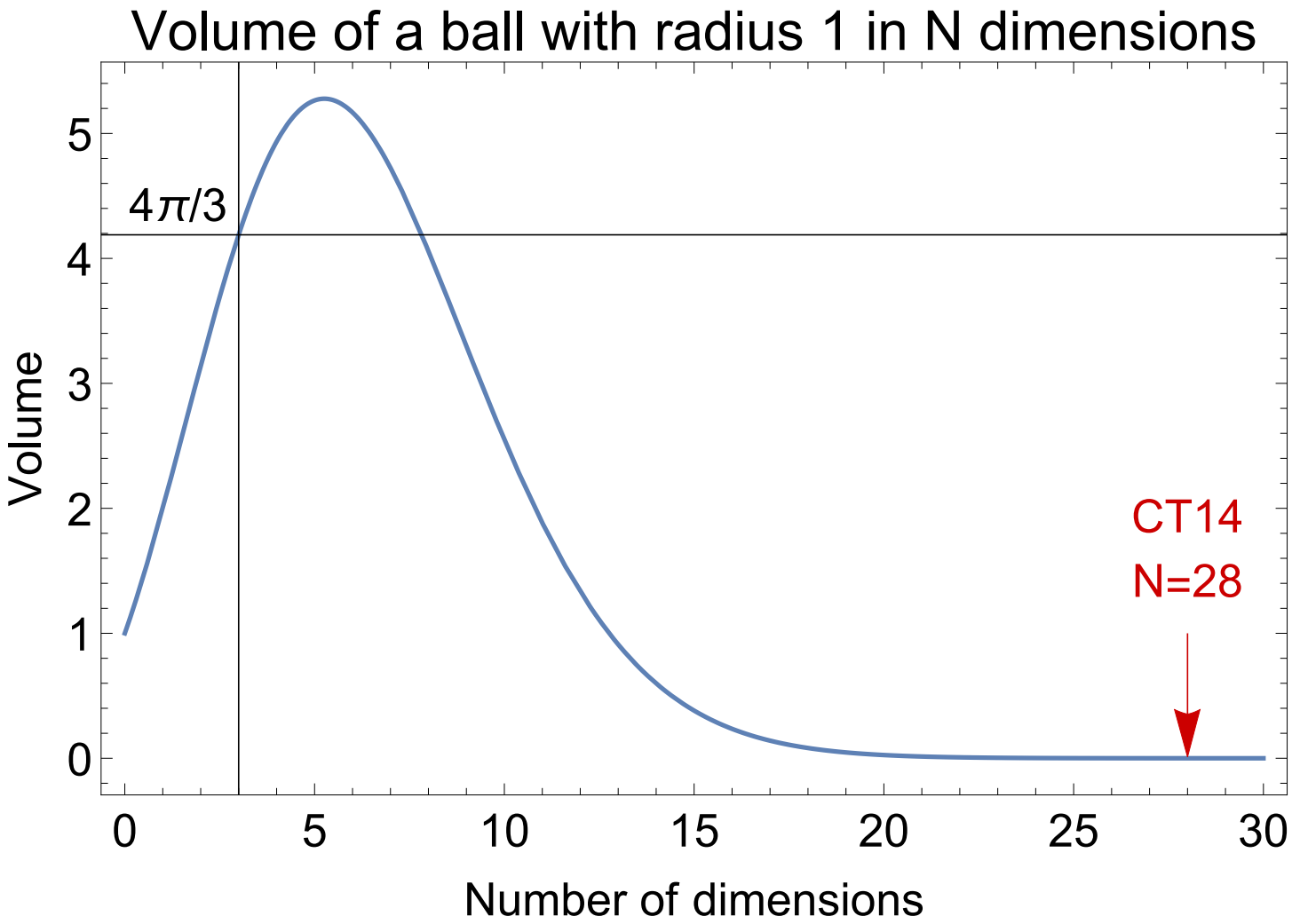

4. Statistical aspects

J. Pumplin et al., JHEP 0207, 012 (2002), and references therein; J. Collins & J. Pumplin, hep-ph/0105207

Say, we must find $N = 28$ PDF parameters $\{a_i\}$ of the CT14 PDF ensemble from N_{exp} experiments with N_k correlated systematic errors in each experiment

Each systematic error is associated with a random parameter r_n, assumed to be distributed as a Gaussian distribution with unit dispersion

The best external estimate of syst. errors corresponds to $\{r_n = 0\}$; but we must allow for $r_n \neq 0$

The most likely combination of $\{a\}$ and $\{r\}$ is found by minimizing

$$\chi^2(\{a\},\{r\}) = \sum_{k=1}^{N_{exp}} w_k \chi^2_k(\{a\},\{r\})$$

$w_k > 0$ are the weights applied to emphasize or de-emphasize contributions from individual experiments (default: $w_k = 1$)

4. Statistical aspects

J. Pumplin et al., JHEP 0207, 012 (2002), and references therein; J. Collins & J. Pumplin, hep-ph/0105207

χ^2 for one experiment is

$$\chi^2_k = \sum_{i=1}^{M_k} \frac{1}{\sigma_i^2} \left(D_i - T_i(\{a\}) - \sum_{n=1}^{R_k} r_n \beta_{ni} \right)^2 + \sum_{n=1}^{R_k} r_n^2$$

D_i and T_i are **data** and **theory** values at each point

$\sigma_i = \sqrt{\sigma^2_{stat} + \sigma^2_{syst,uncor}}$ is the total statistical + systematical **uncorrelated** error

$\sum_n \beta_{ni} r_k$ are **correlated** systematic shifts

β_{ni} is the **correlation** matrix; is provided with the data or theoretical cross sections before the fit

$\sum_n r_n^2$ is the penalty for deviations of r_n from their expected values, $r_n = 0$

Multi-dimensional error analysis

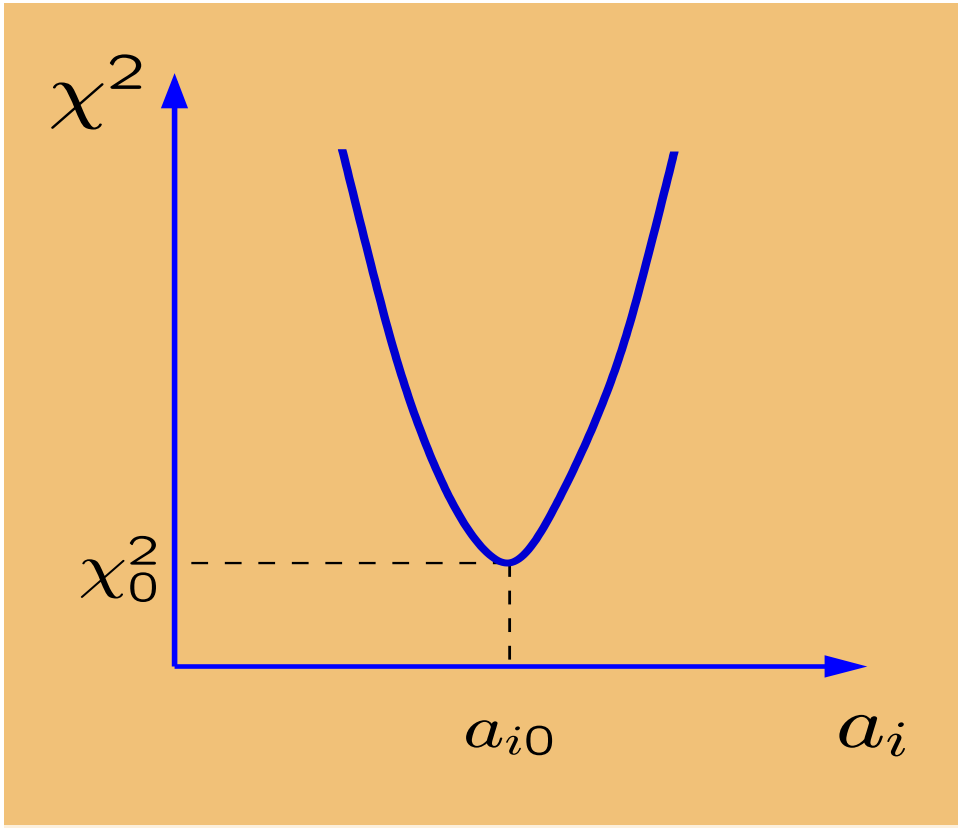

- Minimization of a likelihood function (χ^2) with respect to ~ 40 theoretical (mostly PDF) parameters $\{a_i\}$ and > 300 experimental systematical parameters

Multi-dimensional error analysis

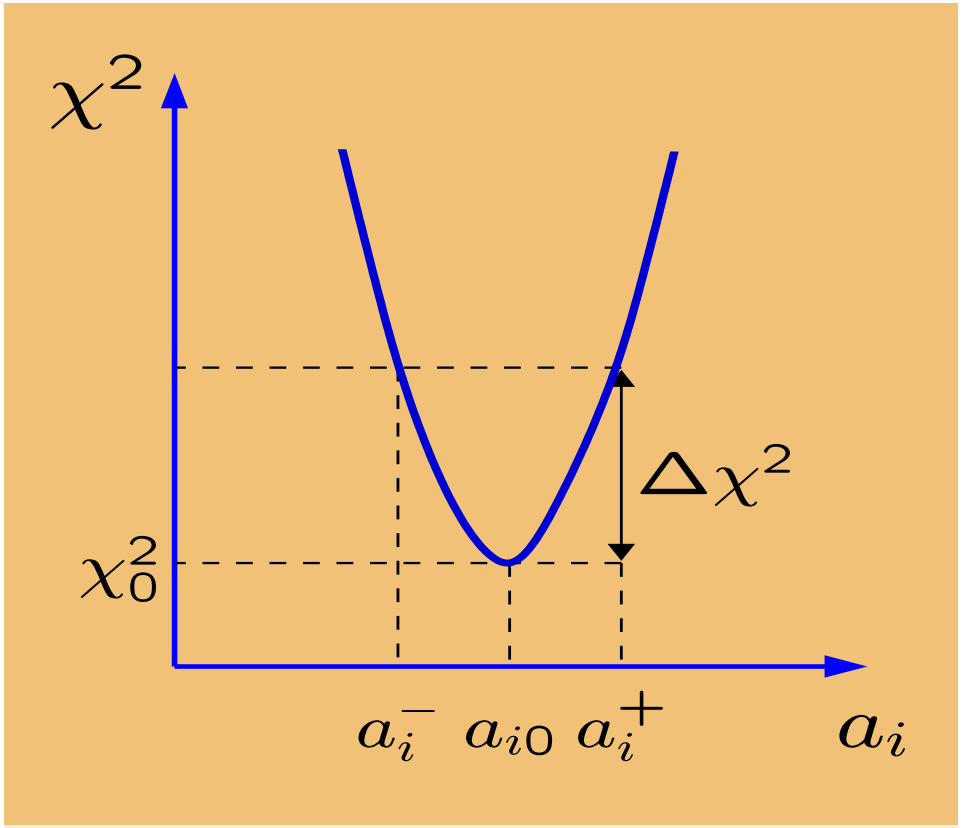

- Establish a confidence region for $\{a_i\}$ for a given tolerated increase in χ^2
- In the ideal case of perfectly compatible Gaussian errors, 68% c.l. on a physical observable X corresponds to $\Delta\chi^2 = 1$ independently of the number N of PDF parameters

See, e.g., P. Bevington, K. Robinson, Data analysis and error reduction for the physical sciences

Multi-dimensional error analysis

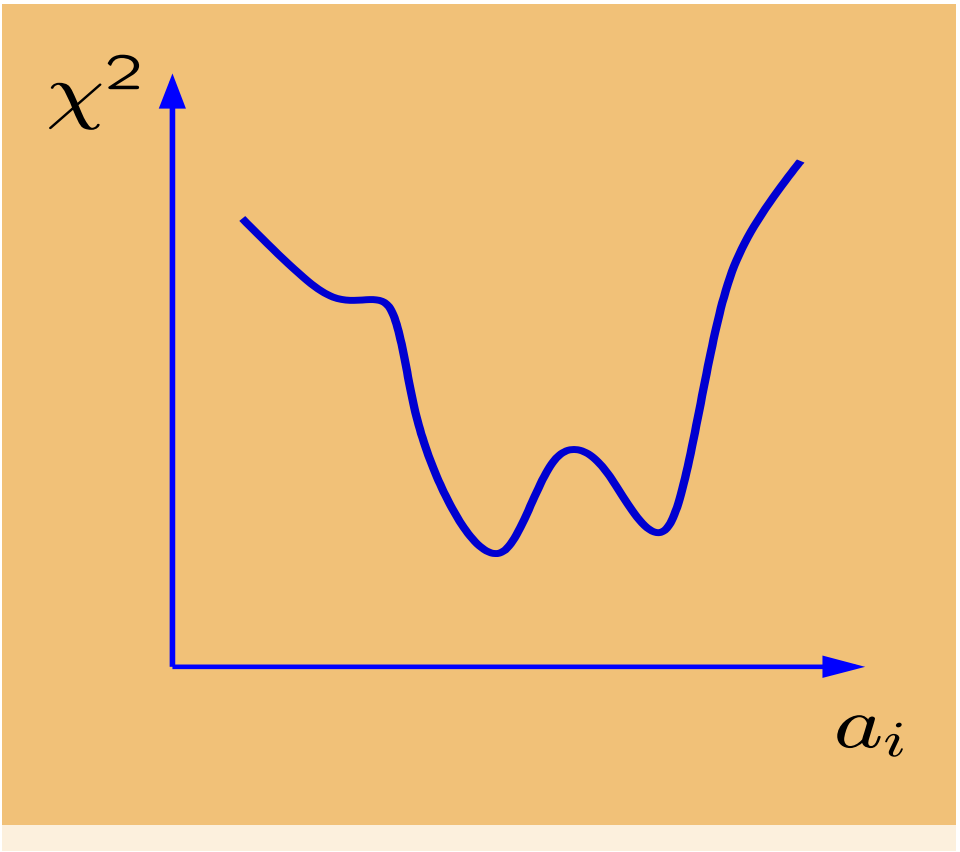

Pitfalls to avoid

- "Landscape"
  - disagreements between the experiments

In the worst situation, significant disagreements between M experimental data sets can produce up to $N \sim M!$ possible solutions for PDF's, with $N \sim 10^{500}$ reached for "only" about 200 data sets

Multi-dimensional error analysis

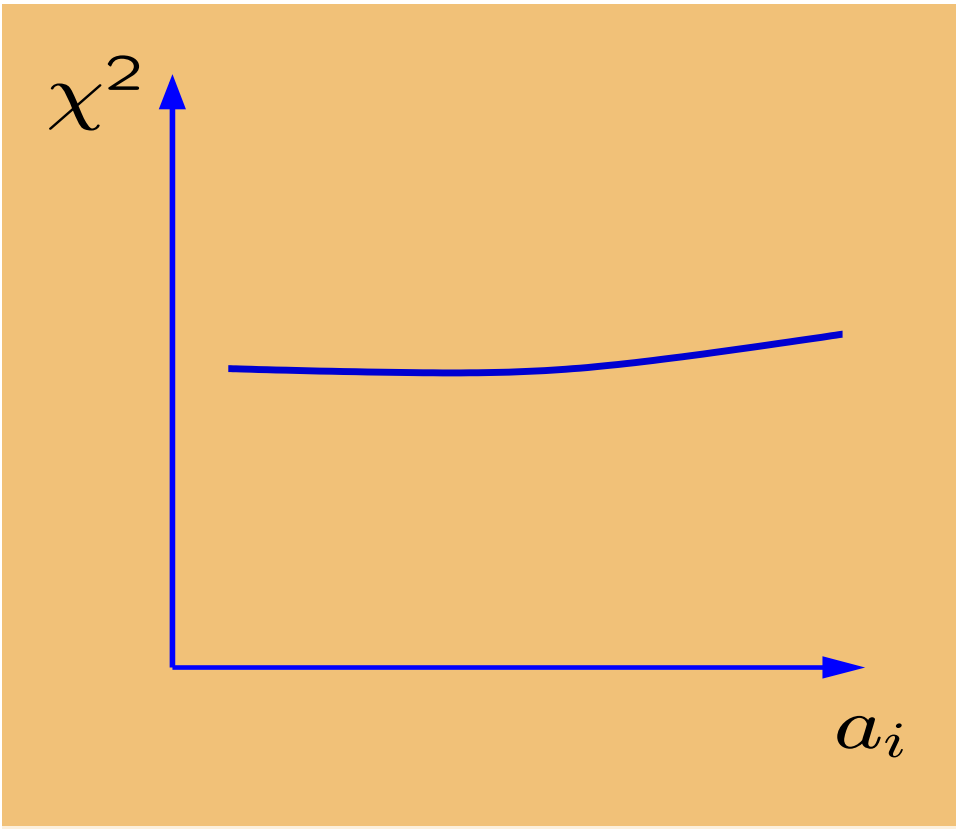

Pitfalls to avoid

- Flat directions
  - unconstrained combinations of PDF parameters
  - dependence on free theoretical parameters, especially in the PDF parametrization
  - impossible to derive reliable PDF error sets

Multi-dimensional error analysis

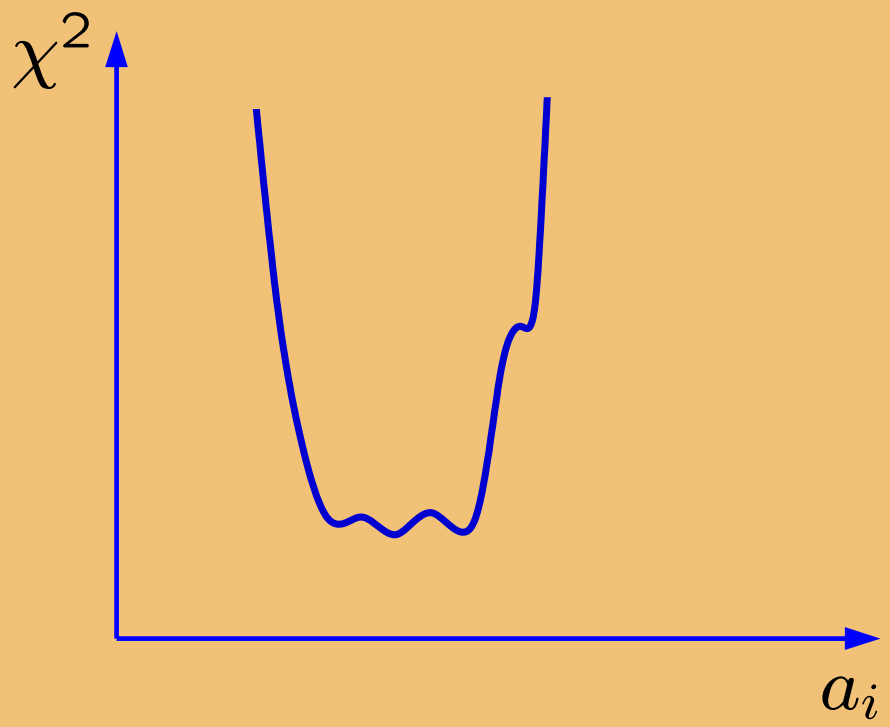

The actual χ^2 function shows

- a well pronounced global minimum χ^2_0
- weak tensions between data sets in the vicinity of χ^2_0 (mini-landscape)
- some dependence on assumptions about flat directions

Multi-dimensional error analysis

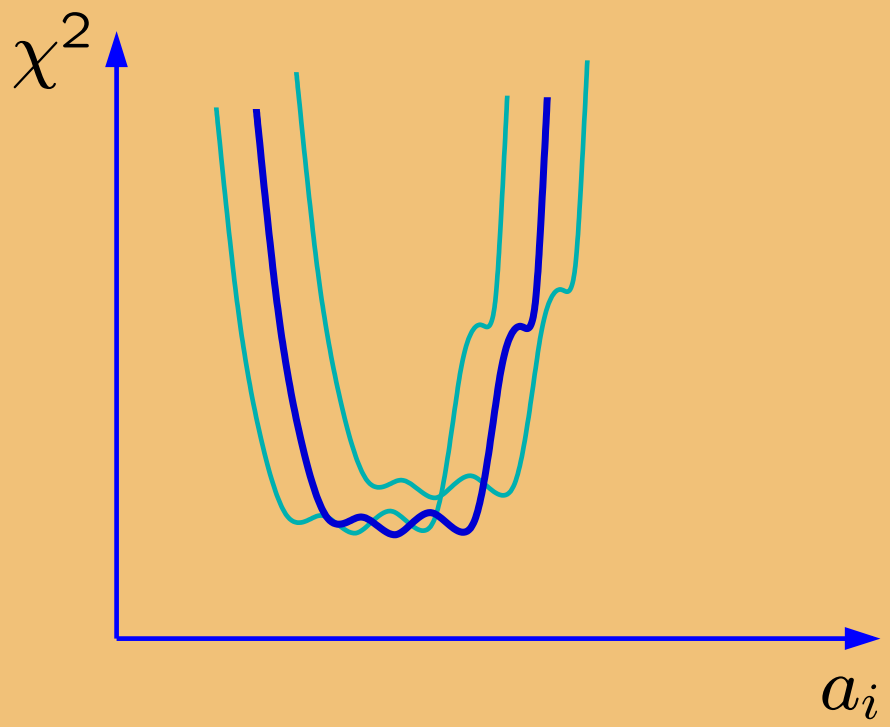

The actual χ^2 function shows

- a well pronounced global minimum χ^2_0
- weak tensions between data sets in the vicinity of χ^2_0 (mini-landscape)
- some dependence on assumptions about flat directions

Multi-dimensional error analysis

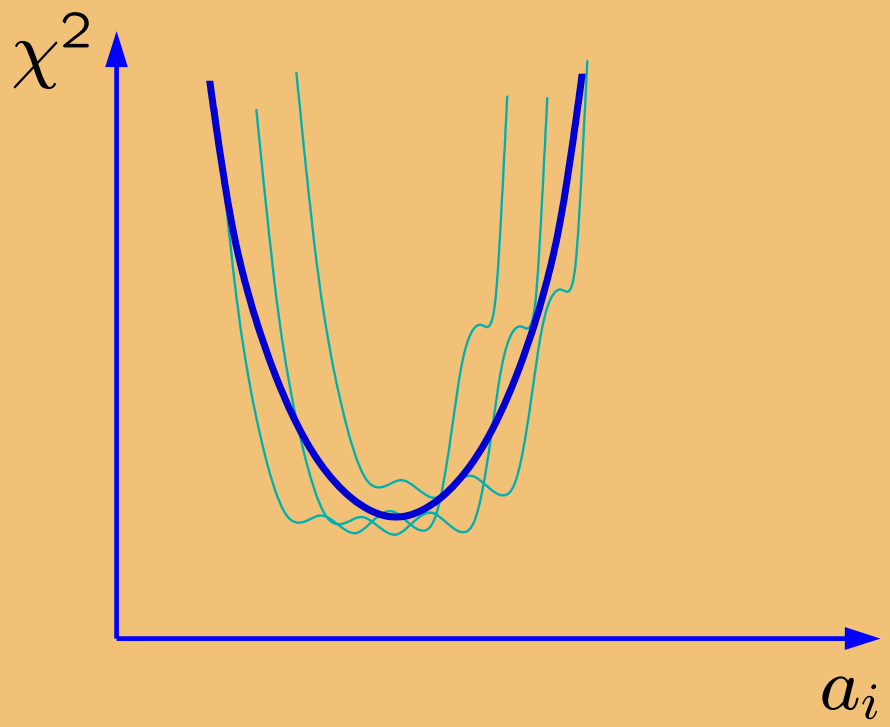

The actual χ^2 function shows

- a well pronounced global minimum χ^2_0
- weak tensions between data sets in the vicinity of χ^2_0 (mini-landscape)
- some dependence on assumptions about flat directions

The likelihood is approximately described by a quadratic χ^2 with a revised tolerance condition $\Delta\chi^2 \leq T^2$

Multi-dimensional error analysis

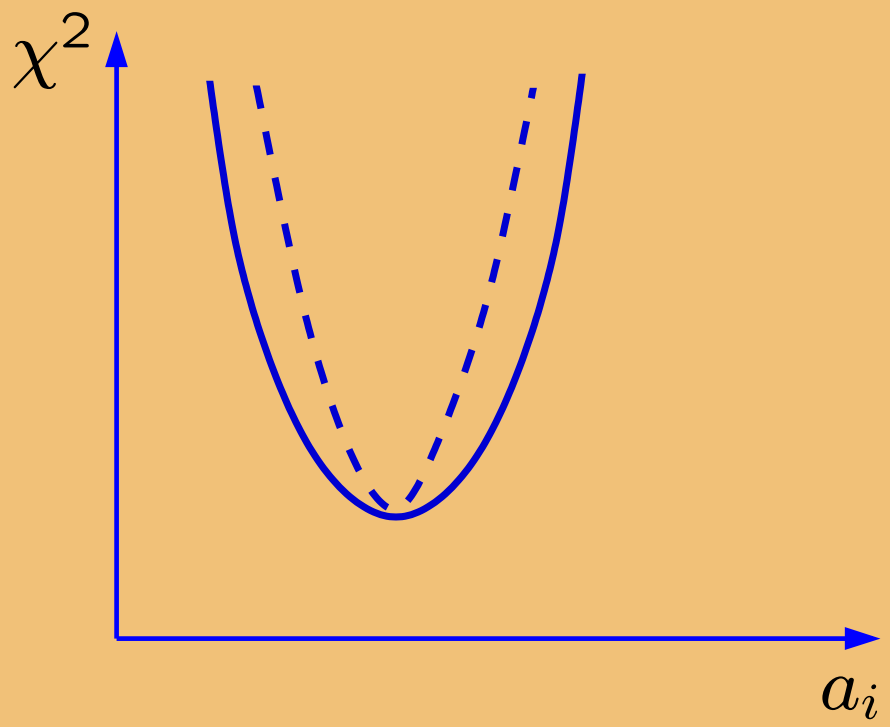

The actual χ^2 function shows

- a well pronounced global minimum χ^2_0
- weak tensions between data sets in the vicinity of χ^2_0 (mini-landscape)
- some dependence on assumptions about flat directions

The likelihood is approximately described by a quadratic χ^2 with a revised tolerance condition $\Delta\chi^2 \leq T^2$

Multi-dimensional error analysis

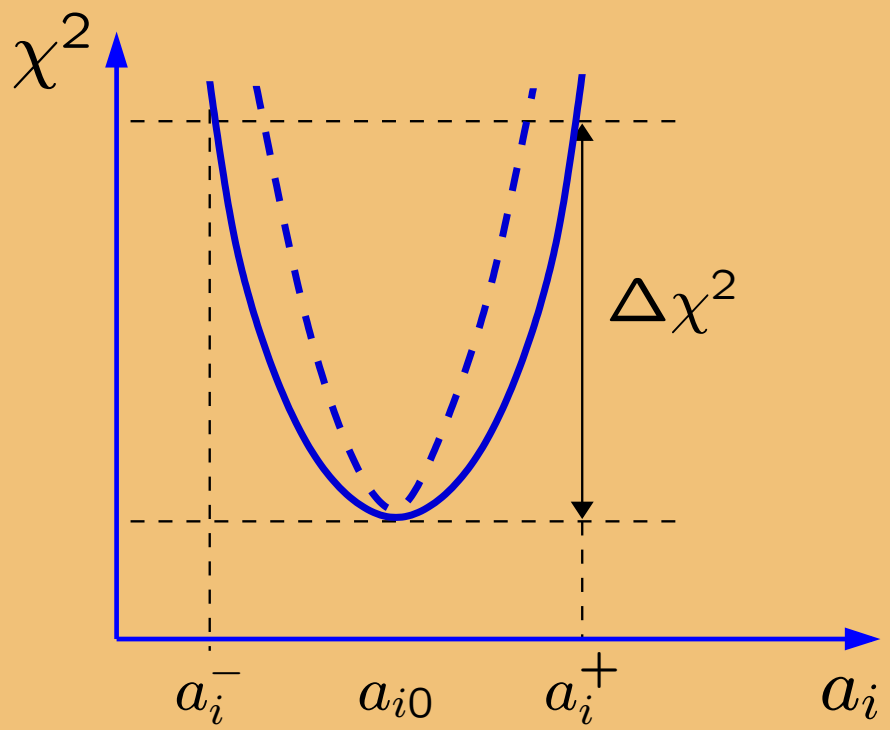

The actual χ^2 function shows

- a well pronounced global minimum χ^2_0
- weak tensions between data sets in the vicinity of χ^2_0 (mini-landscape)
- some dependence on assumptions about flat directions

The likelihood is approximately described by a quadratic χ^2 with a revised tolerance condition $\Delta\chi^2 \leq T^2$

Confidence intervals in a global PDF analysis

Monte-Carlo sampling of the PDF parameter space

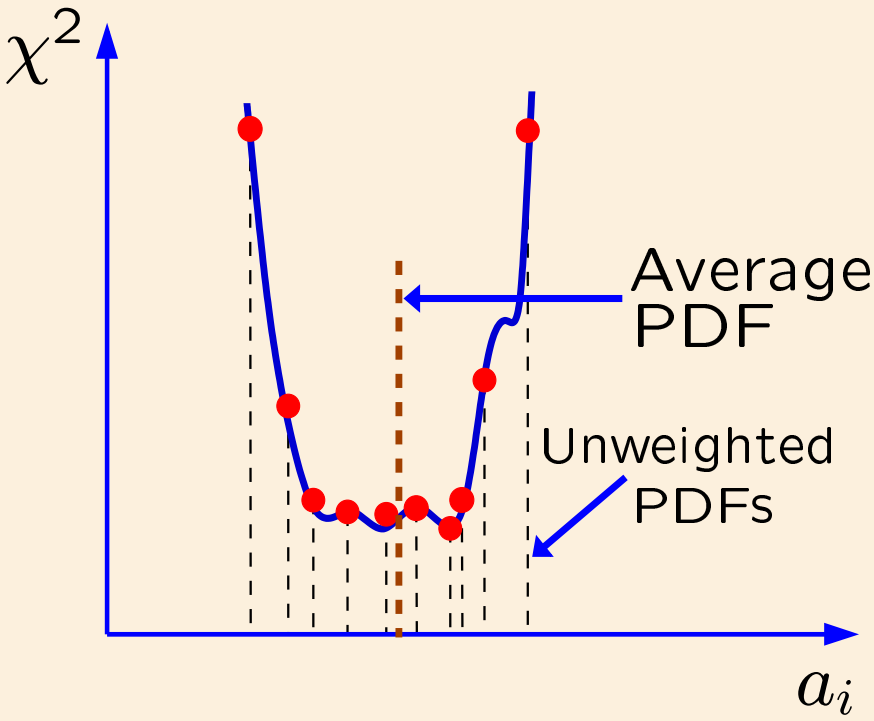

A very general approach that

- realizes stochastic sampling of the probability distribution

(Alekhin; Giele, Keller, Kosower; NNPDF)

- can parametrize PDF's by flexible neural networks (NNPDF)
- does not rely on smoothness of χ^2 or Gaussian approximations

Confidence intervals in a global PDF analysis

Monte-Carlo sampling of the PDF parameter space

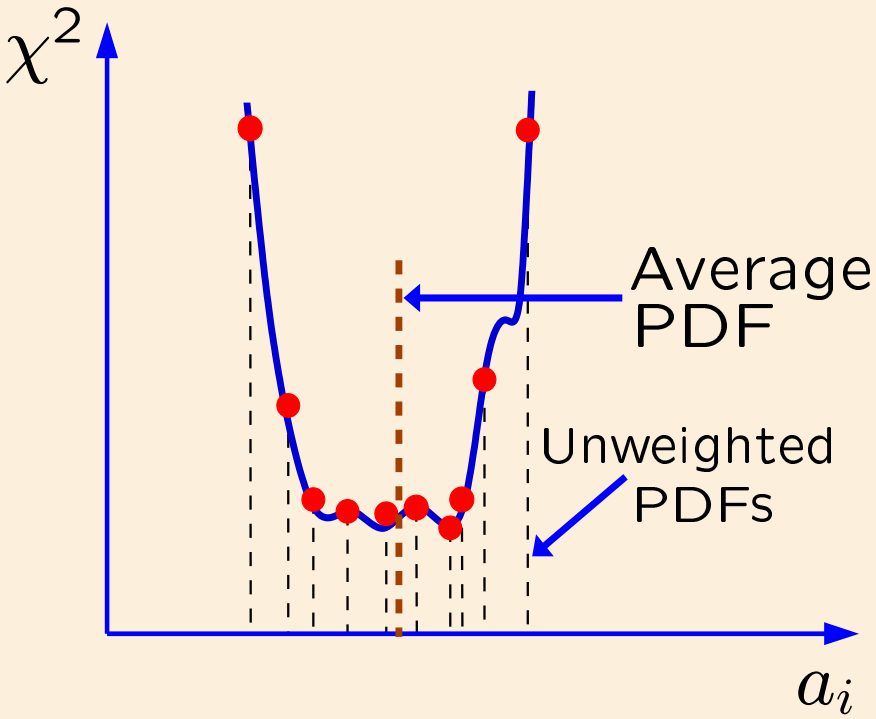

- Most individual replicas are **very bad** fits with $\Delta\chi^2 > 100$ *(1607.06066)*

  Recall that the $\Delta\chi^2 < 100$ ball has almost no volume in $N > 30$ dimensions

- A good fit is obtained by averaging over the replicas

Key formulas of the Hessian method

The Hessian method is used by CTXX PDFs to propagate the PDF uncertainty into QCD predictions.

It provides several simple formulas for computing the PDF uncertainties and PDF-induced correlations.

Tolerance hypersphere in the PDF space

2-dim (i,j) rendition of N-dim (22) PDF parameter space

contours of constant χ^2_{global}

$\mathbf{u}_l$: *eigenvector in the l-direction*

$\mathbf{p}(i)$: *point of largest* a_i *with tolerance* T

$\boldsymbol{s}_0$: *global minimum*

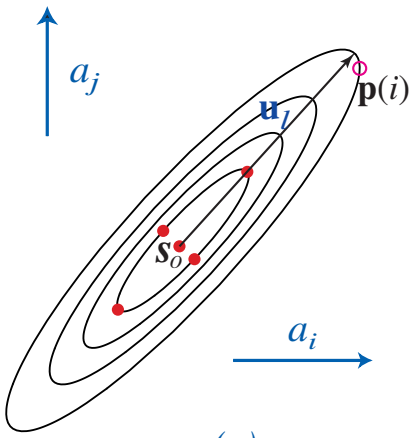

(a)

Original parameter basis

diagonalization and rescaling by the iterative method

- *Hessian eigenvector basis sets*

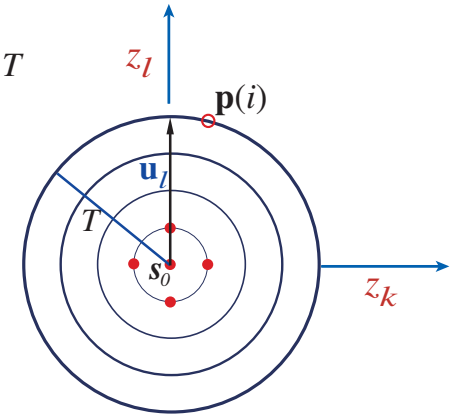

(b)

Orthonormal eigenvector basis

A hyperellipse $\Delta\chi^2 \leq T^2$ in space of N physical PDF parameters $\{a_i\}$ is mapped onto a filled hypersphere of radius T in space of N orthonormal PDF parameters $\{z_i\}$

Tolerance hypersphere in the PDF space

2-dim (i,j) rendition of N-dim (22) PDF parameter space

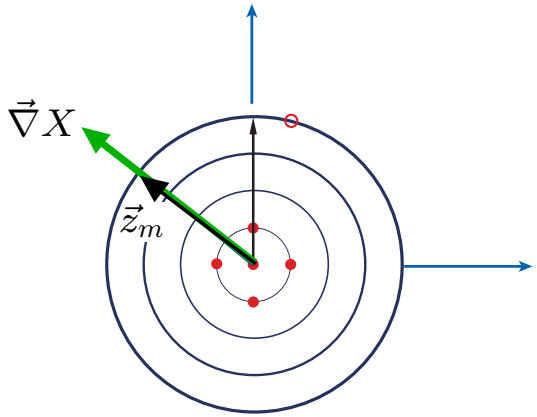

(b)
Orthonormal eigenvector basis

A symmetric PDF error for a physical observable X is given by

$$\Delta X = \vec{\nabla} X \cdot \vec{z}_m = \left|\vec{\nabla} X\right| = \frac{1}{2}\sqrt{\sum_{i=1}^{N}\left(X_i^{(+)} - X_i^{(-)}\right)^2}$$

Asymmetric PDF errors can be also computed.

Tolerance hypersphere in the PDF space

2-dim (i,j) rendition of N-dim (22) PDF parameter space

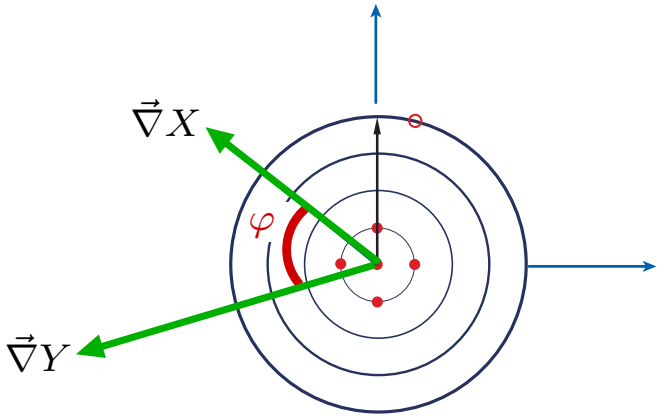

(b)
Orthonormal eigenvector basis

Correlation cosine for observables X and Y:

$$\cos\varphi = \frac{\vec{\nabla}X \cdot \vec{\nabla}Y}{\Delta X \Delta Y} = \frac{1}{4\Delta X\, \Delta Y} \sum_{i=1}^{N} \left(X_i^{(+)} - X_i^{(-)}\right)\left(Y_i^{(+)} - Y_i^{(-)}\right)$$

Sensitivity of PDFs to input cross sections

It is often interesting to know which specific data sets included in the PDF analysis constrain a given $f_{a/p}(x, Q)$; or which PDF flavors drive the PDF uncertainty in a given QCD observable X

This question can be addressed in several ways:

- by computing the correlation cosine $\cos\phi$ in the Hessian method *(Sullivan, PN, 2001; Nadolsky et al., 0802.0007)*
- by a Lagrange multiplier scan of X *(Stump et al., hep-ph/0101051)*
- by introducing effective Gaussian variables S_n *(Dulat et al., 1309.0025, 1310.7601; Lai et al., 1007.2241)*
- using **the sensitivity variable** S_f("correlation 2.0") -> an easy-to-compute indicator of data point sensitivity to PDFs in the presence of experimental errors *(B.T. Wang et al., 1803.02777)*

Statistical methods to identify the PDF dependence

1. PDF-driven correlations with theory cross sections [arXiv:0802.0007]
If the **theory** cross section σ is sensitive to a given PDF f, the Hessian correlation $\cos\varphi$ is close to ± 1

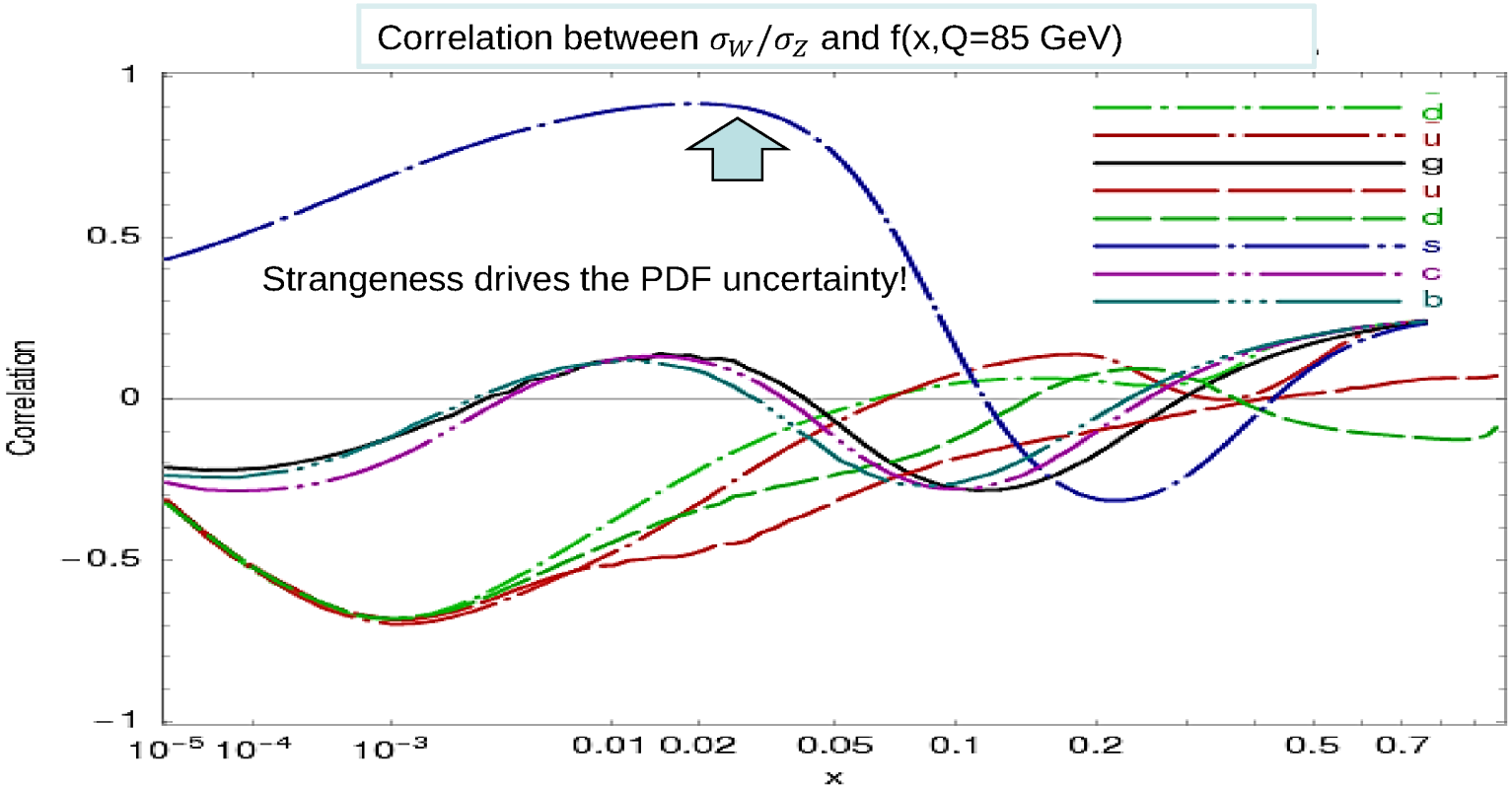

Useful, but incomplete information!

Statistical methods to identify the PDF dependence

2. Sensitivity of a data point
[B.W. Wang, T.J. Hobbs, et al., arXiv:1803.02777; **program PDFSense**]

If a **data point** is sensitive to a given PDF f, then the sensitivity $|S_f|$ of this data point to f is much larger than 0 [say, $|S_f| > 0.25$]. S_f is defined on the next slide.

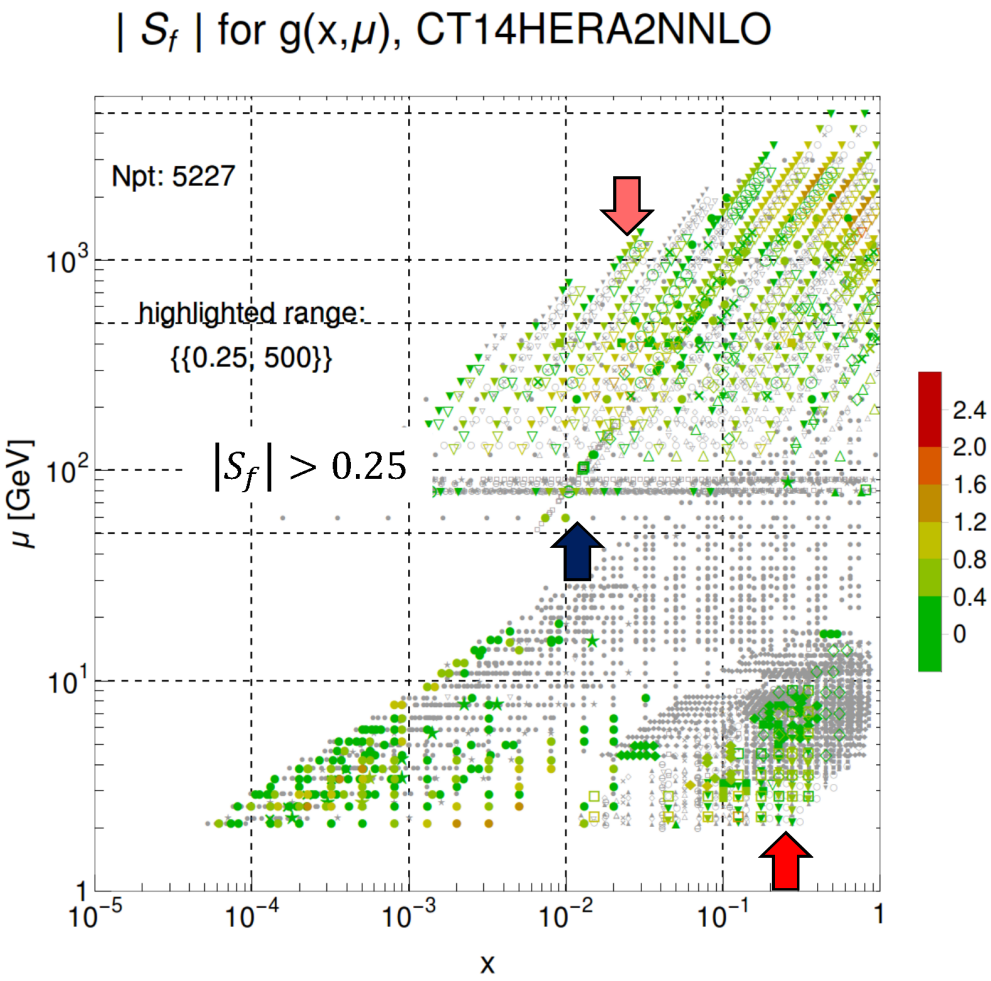

Correlation C_f and sensitivity S_f

The relation of data point i on the PDF dependence of f can be estimated by:

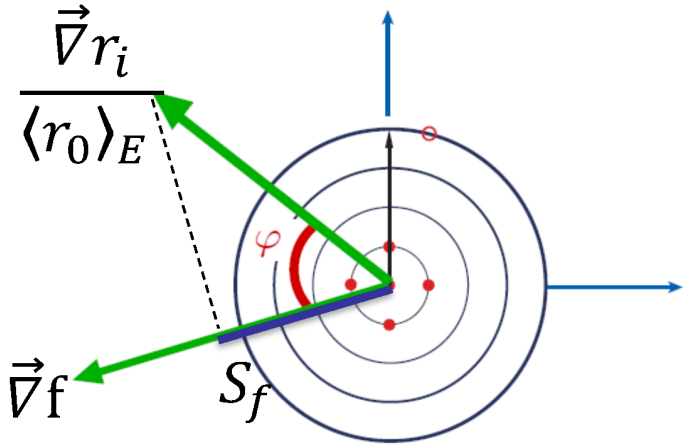

- $C_f \equiv \mathrm{Corr}[\rho_i(\vec{a})), f(\vec{a})] = cos\varphi$

$\vec{\rho}_i \equiv \vec{\nabla} r_i / \langle r_0 \rangle_E$ -- gradient of r_i normalized to the r.m.s. average residual in expt E;

$$(\vec{\nabla} r_i)_k = (r_i(\vec{a}_k^+) - r_i(\vec{a}_k^-))/2$$

C_f is **independent** of the experimental and PDF uncertainties. In the figures, take $|C_f| \gtrsim 0.7$ to indicate a large correlation.

- $S_f \equiv |\vec{\rho}_i| cos\varphi = C_f \frac{\Delta r_i}{\langle r_0 \rangle_E}$ -- projection of $\vec{\rho}_i(\vec{a})$ on $\vec{\nabla} f$

S_f is proportional to $\cos\varphi$ and the ratio of the PDF uncertainty to the experimental uncertainty. We can sum $|S_f|$.
In the figures, take $|S_f| > 0.25$ to be significant.

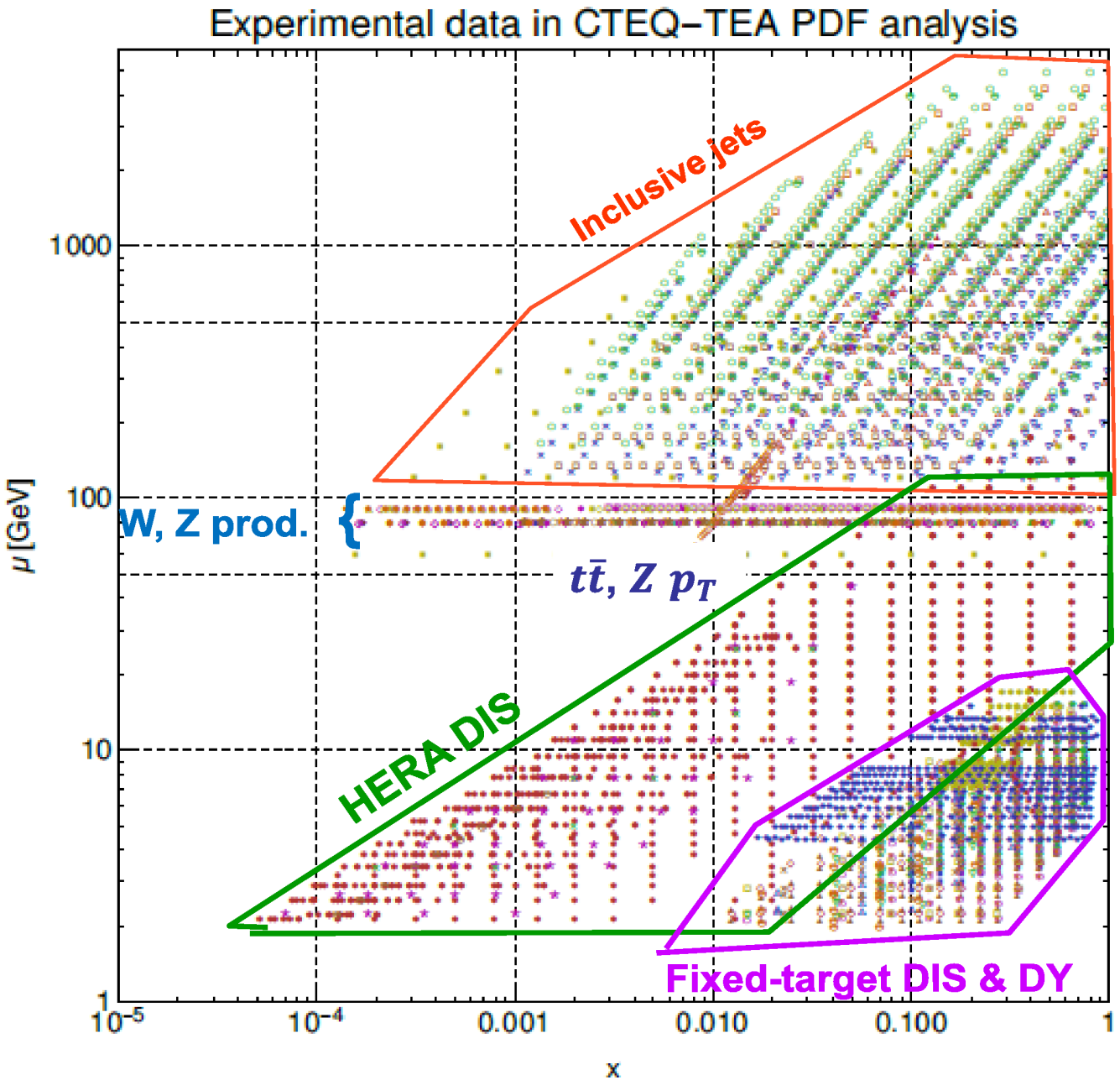
Experimental data in CTEQ–TEA PDF analysis
Inclusive jets
W, Z prod.
$t\bar{t}$, Z p_T
HERA DIS
Fixed-target DIS & DY
1000
100
10
1
μ [GeV]
10^{-5}
10^{-4}
0.001
0.010
0.100
1
x

$|S_f|$ for g(x,μ), CT14HERA2NNLO

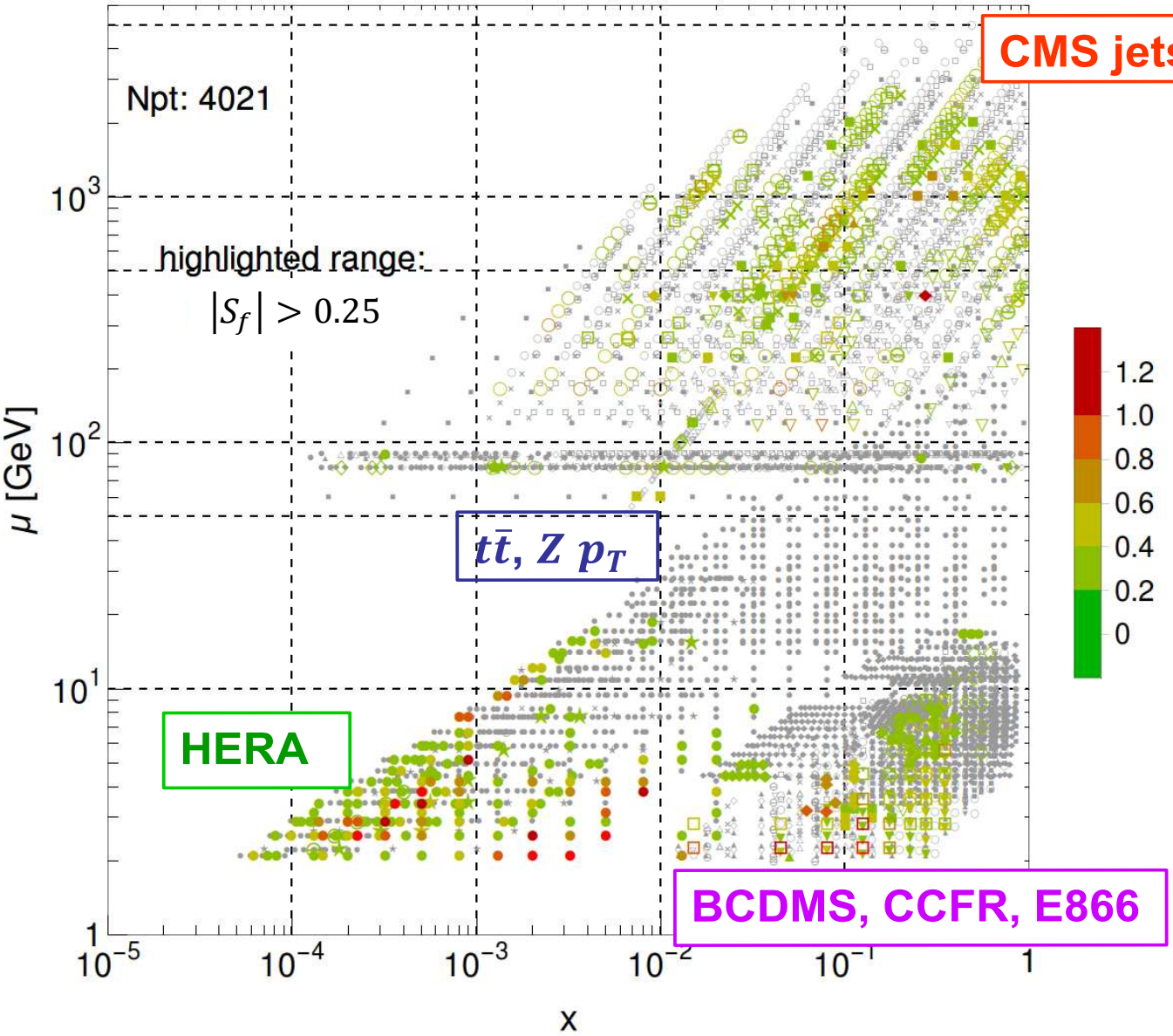

Experiments with the highest sensitivity to $g(x_i, \mu_i)$

Not all these experiments have high correlation with $g(x, \mu)$!

HERA DIS, fixed-target DIS, jets have comparable total sensitivities

Higgs boson production

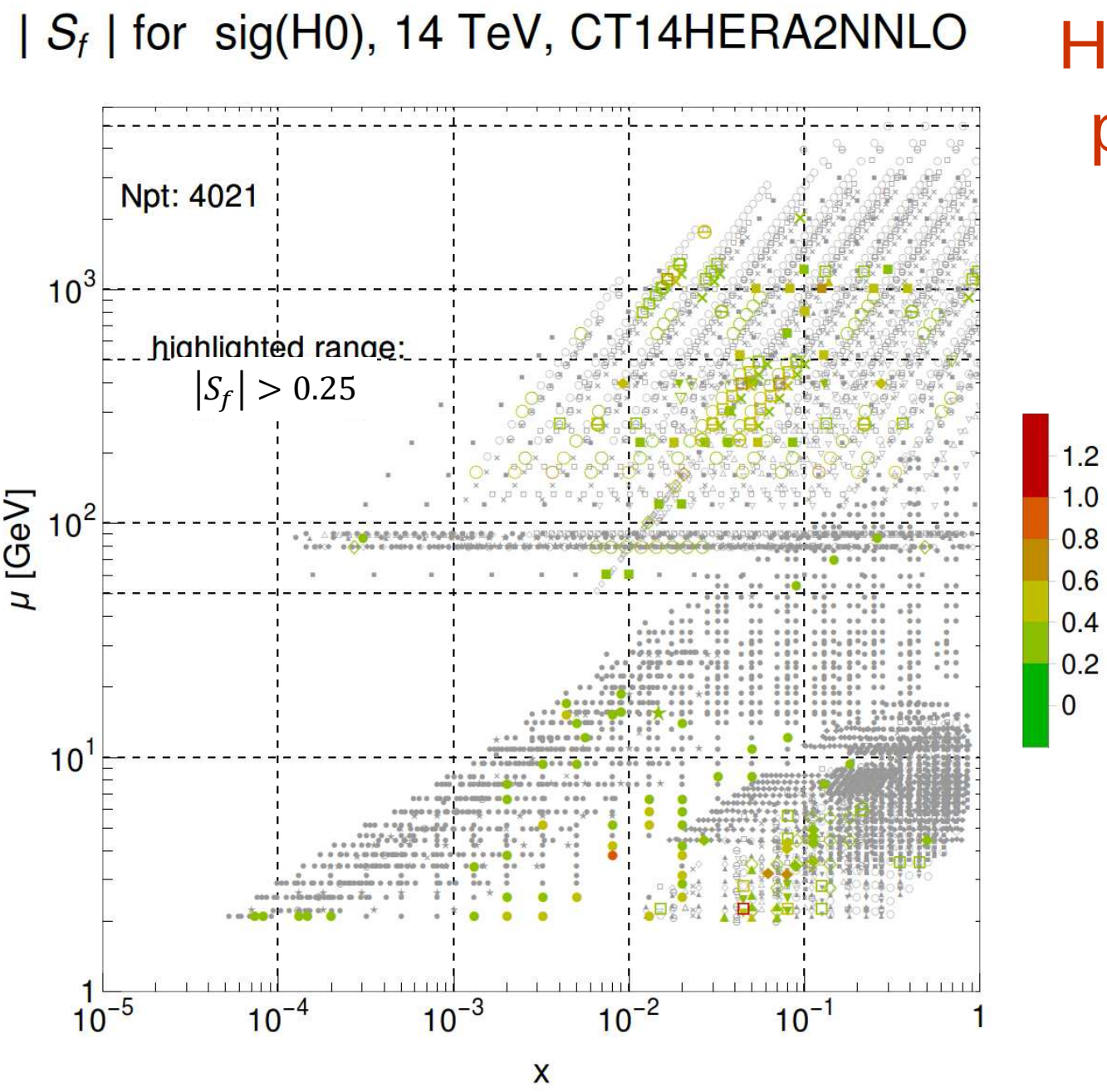

HERA DIS still has the dominant sensitivity!

CMS 8 TeV jets is the next sensitive expt.after HERA for $\sigma_H(14\ \text{TeV})$; jet scale uncertainty dampens $|S_f|$ for jets

Good correlations with some points in E866, BCDMS, CCFR, CMS WASY, $Z\ p_T$ and $t\bar{t}$ production; but not as many points with high $|S_f|$ in these processes

Higgs boson production

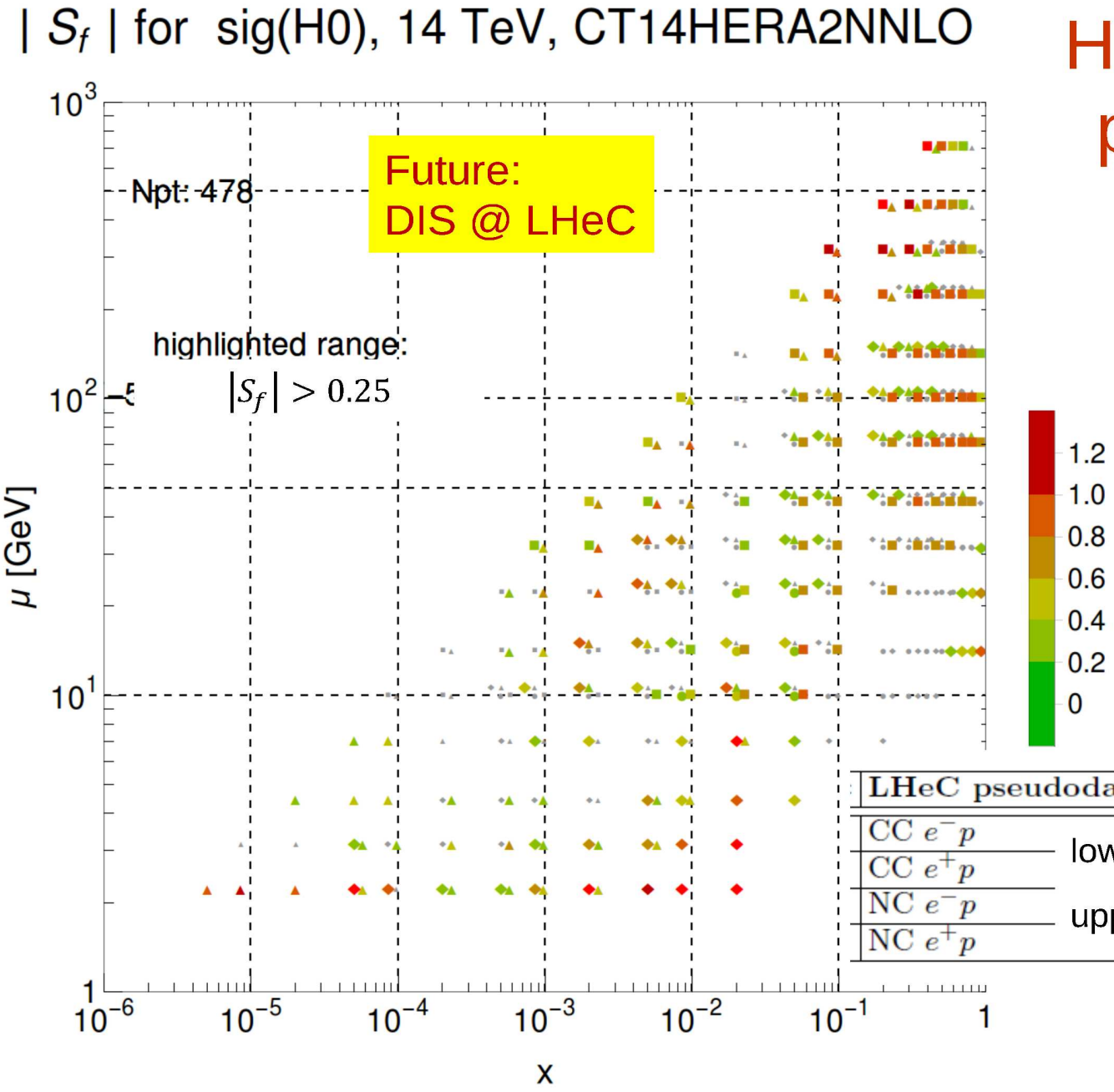

LHeC pseudodata from M. Klein and V. Radescu ($\sqrt{s} = 0.49, 1.3$ TeV; $L = 0.1\ ab^{-1}$; 1 year of running)

LHeC pseudodata set		N_{pt}	Fig. 8 symbol
CC e^-p	lower	93	circle
CC e^+p		109	square
NC e^-p	upper	128	diamond
NC e^+p		148	triangle

$|S_f|$ for $\bar{d}/\bar{u}(x,\mu)$, CT14HERA2NNLO

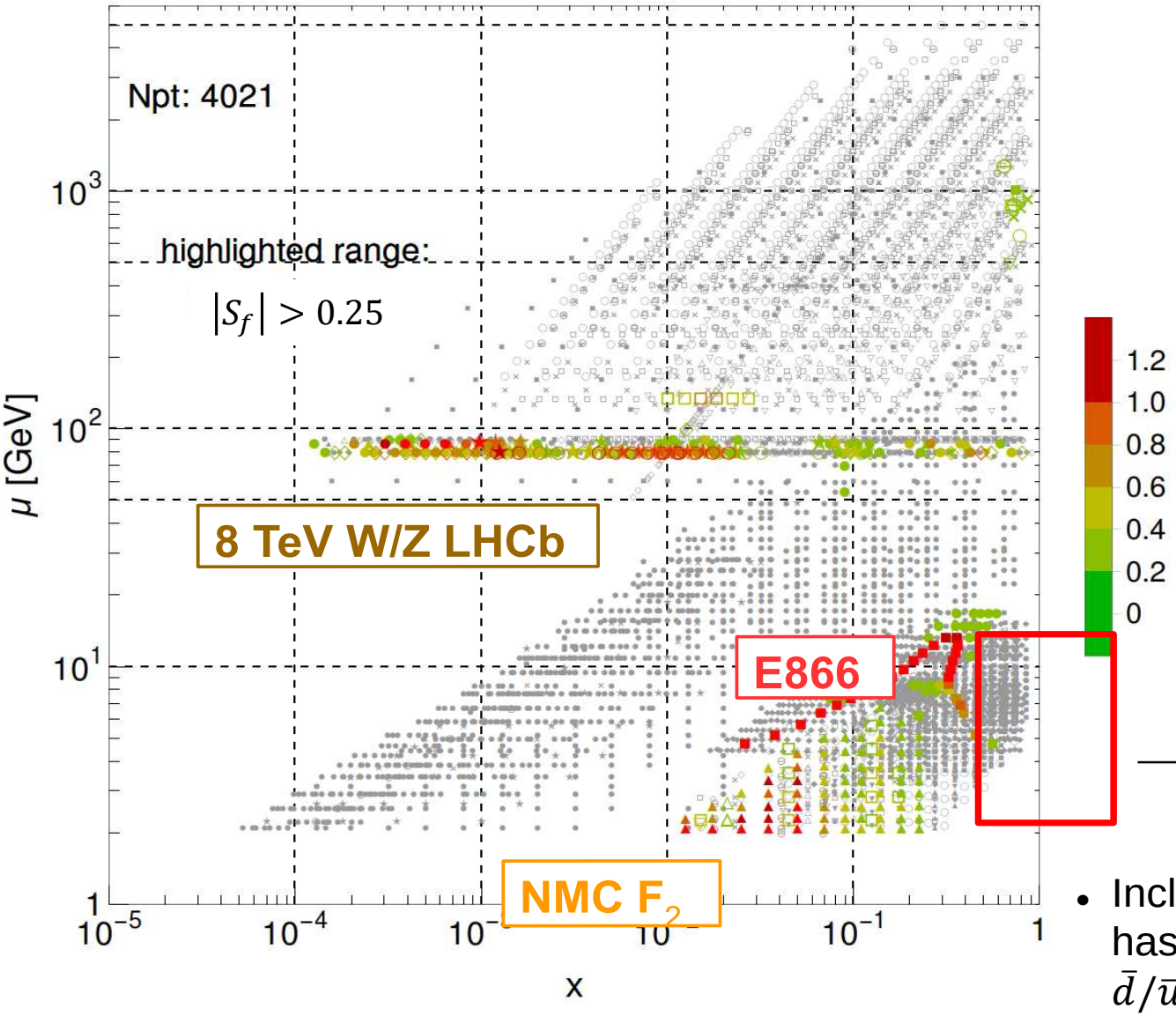

- PDF ratio is sensitive to flavor symmetry breaking in the light quark sea
- the large E866 pd/pp sensitivity *degrades* at larger x
- this is a prime motivation for higher x DY measurements at **E906** (SeaQuest)
- Inclusive jet production has potential to constrain $\bar{d}/\bar{u}$ in the near future

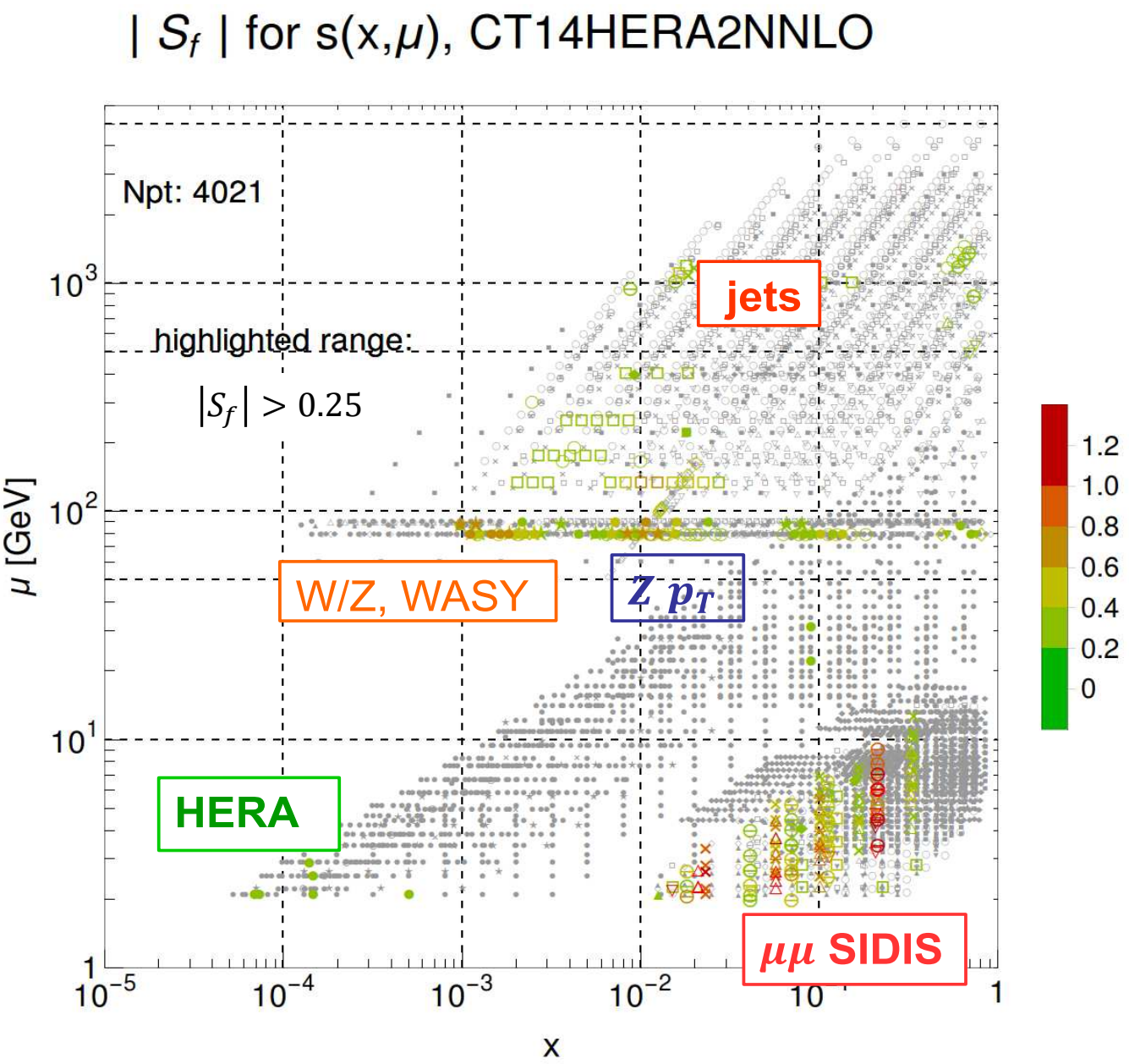

- Points with a large S_f have a stronger sensitivity to $s(x_i, \mu_i)$
- Constraints on $s(x, \mu)$ are weaker than on the other flavors

NuTeV, CCFR dimuon SIDIS, HERA DIS most sensitive

- Combined $|S_f|$ of CMS7+8 jet data comparable to $|S_f|$ of one of NuTeV, CCFR data sets

- W ASYmmetry, σ_W, σ_Z are weakly sensitive

Visualizing LHeC constraints

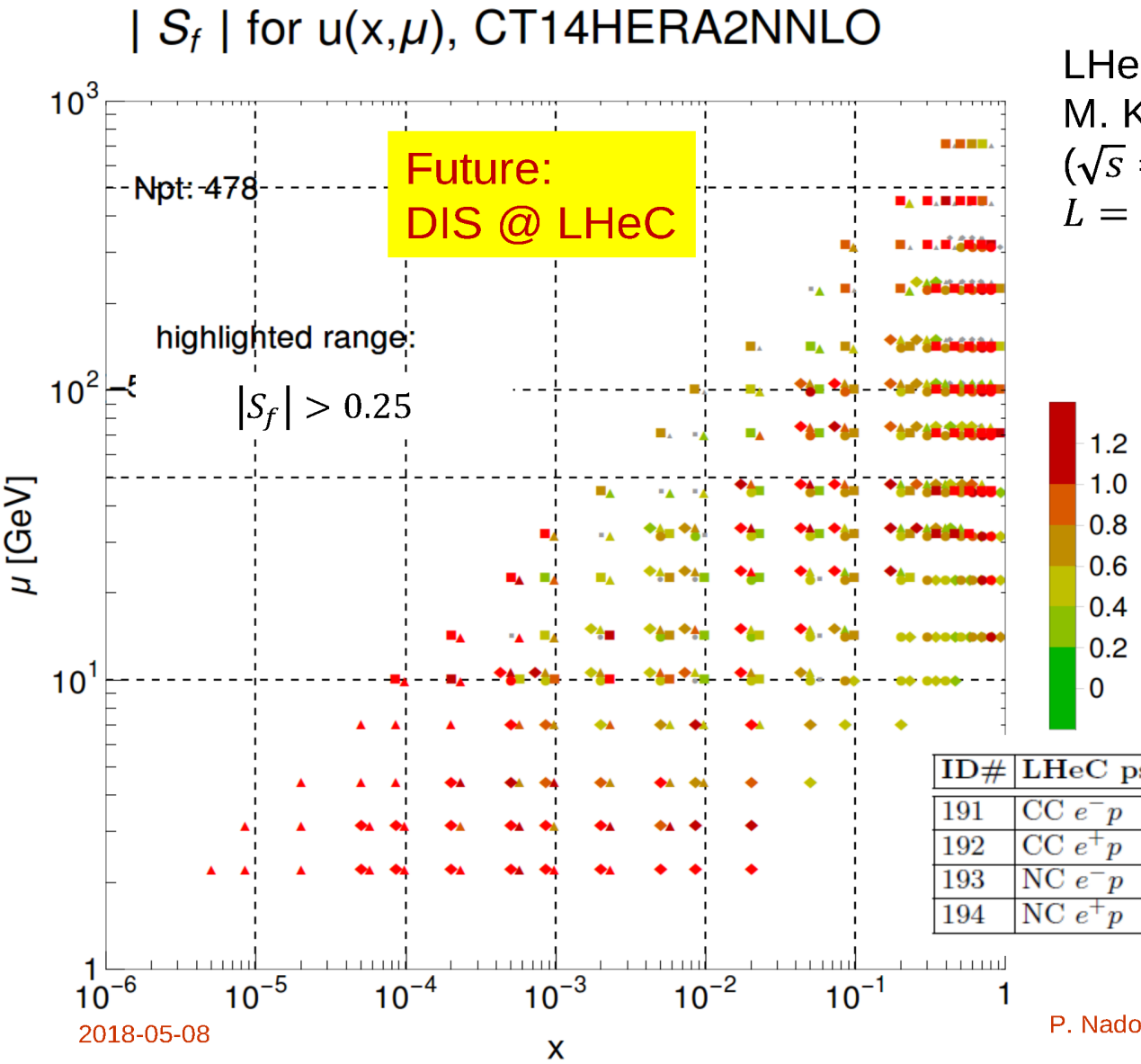

LHeC pseudodata from
M. Klein and V. Radescu
($\sqrt{s} = 0.49, 1.3$ TeV;
$L = 0.1\ ab^{-1}$; 1 year of running)

ID#	LHeC pseudodata set		N_{pt}	Fig. 8 symbol
191	CC e^-p	lower	93	circle
192	CC e^+p	lower	109	square
193	NC e^-p	upper	128	diamond
194	NC e^+p	upper	148	triangle

Visualizing LHeC constraints

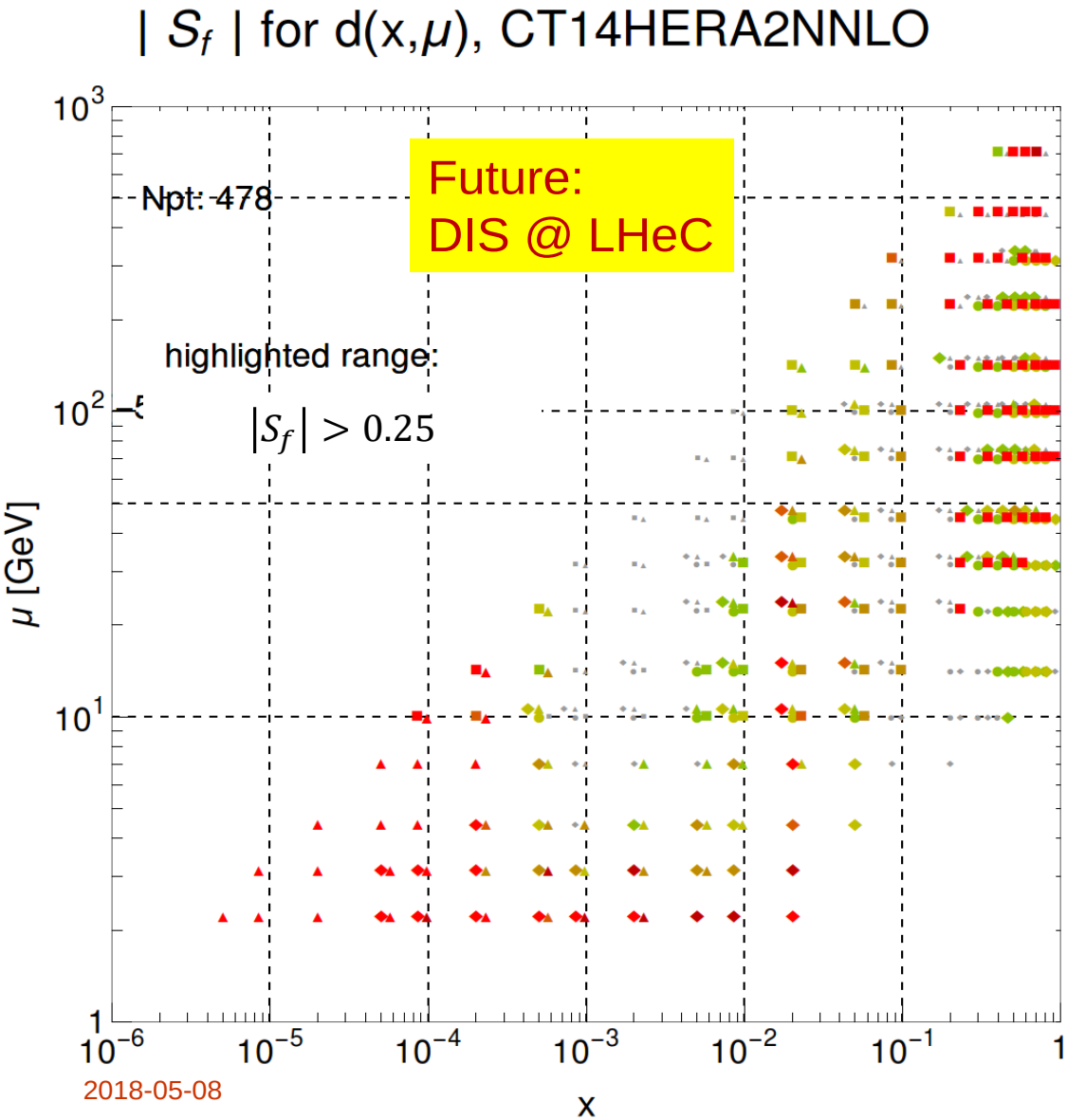

Exceptional sensitivity in CC DIS to $d(x)$ at $x \to 1$!

Great potential to constrain $d(x)/u(x)$ at $x \to 1$, $\langle x \rangle_{u^+ - d^+}$ for lattice QCD comparisons

P. Nadolsky, Pheno'2018

Visualizing LHeC constraints

| S_f | for s(x,μ), CT14HERA2NNLO

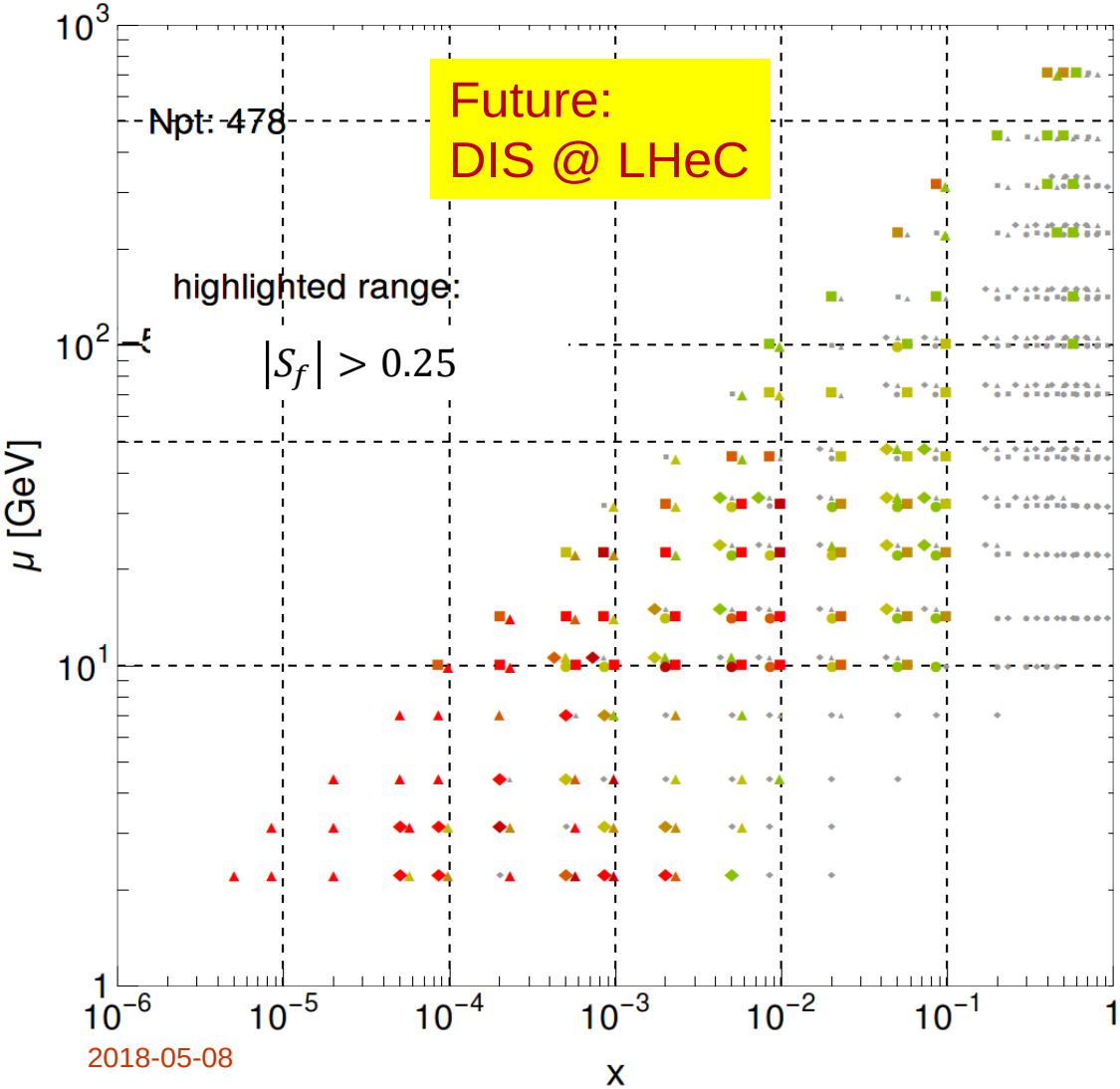

Some sensitivity to $s(x,\mu)$ at $x < 0.1$, $\mu < 40$ GeV

Current data are insensitive to $T_3(x,\mu)$ and $T_8(x,\mu)$ at $x < 10^{-3}$, $Q < 10$ GeV

⇒ All u, d, s (anti)quark S_f are roughly the same at such $\{x, Q\}$

P. Nadolsky, Pheno'2018

Conclusion
Present and future of the PDF analysis

Oekumene of the PDF universe

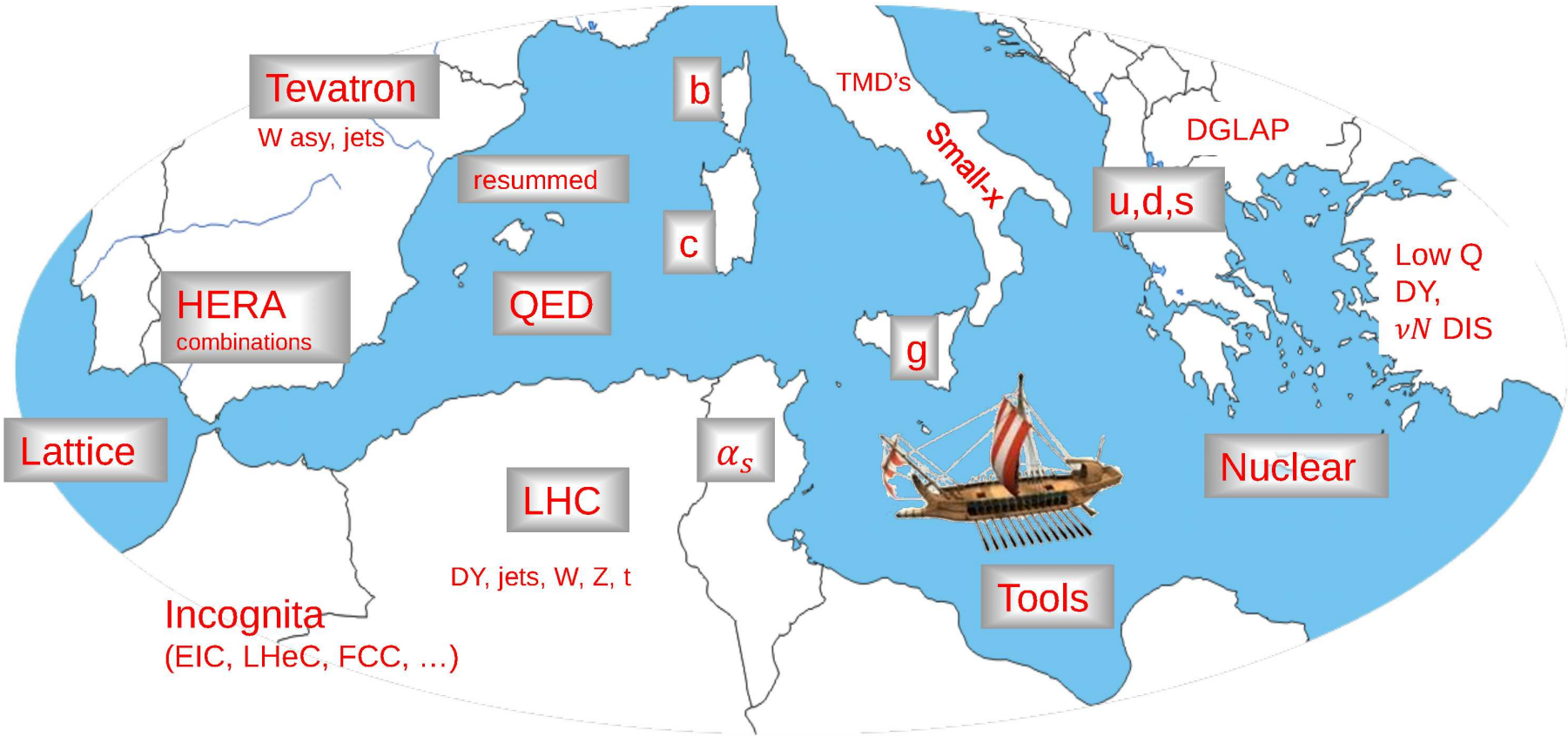

It is a payoff decade for the PDF analysis efforts!

- A windfall of new data to compare with (LHC, HERA, Tevatron, JLab, RHIC,...)
- Tests of QCD factorization at new $\sqrt{s}$, targeting 1% precision
- New tools (HERA Fitter, APPLGRID, FastNLO,...) and methods (MC sampling, PDF reweighting) revolutionize the PDF analysis
- Understanding of the PDFs at the (N)NNLO level will be crucial for the success of the LHC physics program

If you get entangled in the PDFs, read this:

OUTP-15-17P
SMU-HEP-15-12
TIF-UNIMI-2015-14
LCTS/2015-27

PDF4LHC recommendations for LHC Run II

Jon Butterworth[1], Stefano Carrazza[2], Amanda Cooper-Sarkar[3], Albert De Roeck[4,5], Joël Feltesse[6], Stefano Forte[2], Jun Gao[7], Sasha Glazov[8], Joey Huston[9], Zahari Kassabov[2,10], Ronan McNulty[11], Andreas Morsch[4], Pavel Nadolsky[12], Voica Radescu[13], Juan Rojo[14] and Robert Thorne[1].

[1] *Department of Physics and Astronomy, University College London, Gower Street, London WC1E 6BT, UK.*
[2] *TIF Lab, Dipartimento di Fisica, Università di Milano and INFN, Sezione di Milano, Via Celoria 16, I-20133 Milano, Italy*
[3] *Particle Physics, Department of Physics, University of Oxford, 1 Keble Road, Oxford OX1 3NP, UK.*
[4] *PH Department, CERN, CH-1211 Geneva 23, Switzerland*
[5] *Antwerp University, B2610 Wilrijk, Belgium*
[6] *CEA, DSM/IRFU, CE-Saclay, Gif-sur-Yvette, France*
[7] *High Energy Physics Division, Argonne National Laboratory, Argonne, Illinois 60439, U.S.A.*
[8] *Deutsches Elektronen-Synchrotron (DESY), Notkestrasse 85, D-22607 Hamburg, Germany.*
[9] *Department of Physics and Astronomy, Michigan State University, East Lansing, MI 48824 U.S.A.*
[10] *Dipartimento di Fisica, Università di Torino and INFN, Sezione Via Pietro Giuria 1, I-10125 Torino, Italy*
[11] *School of Physics, University College Dublin Science Centre UCD Belfeld, Dublin 4, Ireland*
[12] *Department of Physics, Southern Methodist University, Dallas, TX 752*
[13] *Physikalisches Institut, Universität Heidelberg, Heidelberg, Ge*
[14] *Rudolf Peierls Centre for Theoretical Physics, 1 Keble Ro University of Oxford, OX1 3NP Oxford, UK*

A major revision of the previous PDF4LHC recommendation in arxiv:1101.0538, arXiv:1211.5142

PDF4LHC publication, topics

1. **Review of updates on PDFs from various groups**

NNLO Global PDF sets: CT14, MMHT'14, NNPDF3

PDFs using other methodologies: ABM'12, CJ15, HERAPDF2.0

2. Average PDF sets by PDF4LHC group: PDF4LHC15_30, _100, _MC

Criteria for combination

$\alpha_s(M_Z) = 0.1180 \pm 0.0015$ at 68% c.l.

3. Recommendation on selecting PDF sets for various LHC applications

A. New physics searches

B. Precision tests of SM and PDFs

C. Monte-Carlo simulations

D. Acceptance estimates

Average PDF sets **can** be used **for bulk of applications** in A, C, D

Have fun with using the PDFs in your calculations!

Backup slides

CT14: parametrization forms

- Candidate CT14 fits have 30-35 free parameters
- In general, $f_a(x, Q_0) = A x^{a_1} (1-x)^{a_2} P_a(x)$
- **CT10** assumed $P_a(x) = \exp\left(a_0 + a_3\sqrt{x} + a_4 x + a_5 x^2\right)$
  - exponential form conveniently enforces positive definite behavior
  - but power law behaviors from a_1 and a_2 may not dominate
- In **CT14**, $P_a(x) = G_a(x) F_a(z)$; $G_a(x)$ is a smooth factor
  - $z = 1 - 1\left(1-\sqrt{x}\right)^{a_3}$ preserves desired Regge-like behavior at low x and high x (with $a_3 > 0$)
- Express $F_a(z)$ as a linear combination of Bernstein polynomials:

$$z^4, 4z^3(1-z), 6z^2(1-z)^2, 4z(1-z)^3, (1-z)^4$$

  - each basis polynomial has a single peak, with peaks at different values of z; reduces correlations among parameters

(N+1)-dim. perspective eliminates wrong N-dim. solutions

What about $s(x,Q) \neq \bar{s}(x,Q)$?

This can be tested in subprocesses

$$W^+ s \to c \text{ and } W^- \bar{s} \to \bar{c}$$

In the experiment, charm quarks can be identified by their semileptonic decays,

$$c \to s\mu^+\nu \text{ and } \bar{c} \to \bar{s}\mu^-\bar{\nu}$$

So one sees

$$\nu N \to \mu^- cX \to \mu^-\mu^+ X$$
$$\bar{\nu} N \to \mu^+ cX \to \mu^+\mu^- X$$

— SIDIS muon pair production (NuTeV)

Total strangeness and strangeness asymmetry

Denote

$$[q_i](Q) \equiv \int_0^1 x\, q_i(x,Q)\, dx$$ —net moment fraction carried by q_i

and introduce $s^{\pm}(x) = s(x) \pm \bar{s}(x)$ (total strangeness and its asymmetry). It is possible that

$$\int_0^1 s^-(x)dx = 0$$

(a proton has no net strangeness), but

$$[S^-] \equiv \int_0^{-1} x s^-(x)dx \neq 0$$

(s and $\bar{s}$ have different x distributions)

A large non-vanishing $[S^-]$ might explain "the NuTeV weak angle anomaly"

CCFR (inclusive νN DIS) and NuTeV (SIDIS dimuon production): constraints on strangeness

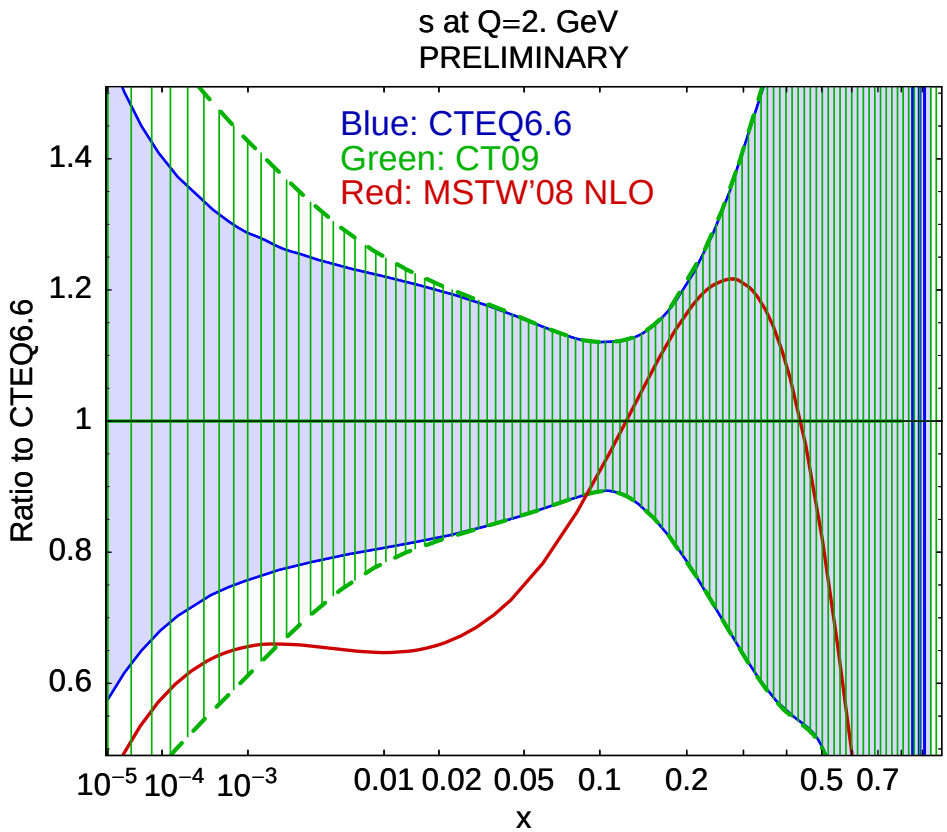

$s^+(x,Q)$ is reasonably well constrained at $x > 0.01$; practically unknown at $x < 0.01$

2009 NNPDF estimate (least biased by the parametrization of $s^-(x,Q)$):

$$[S^-](Q^2 = 20\ \text{GeV}^2) = 0 \pm 0.009$$

No statistically significant $[S^-]$; but the PDF error is large enough to eliminate the NuTeV anomaly (!)

Constraining strangeness PDF by LHC W and Z cross sections

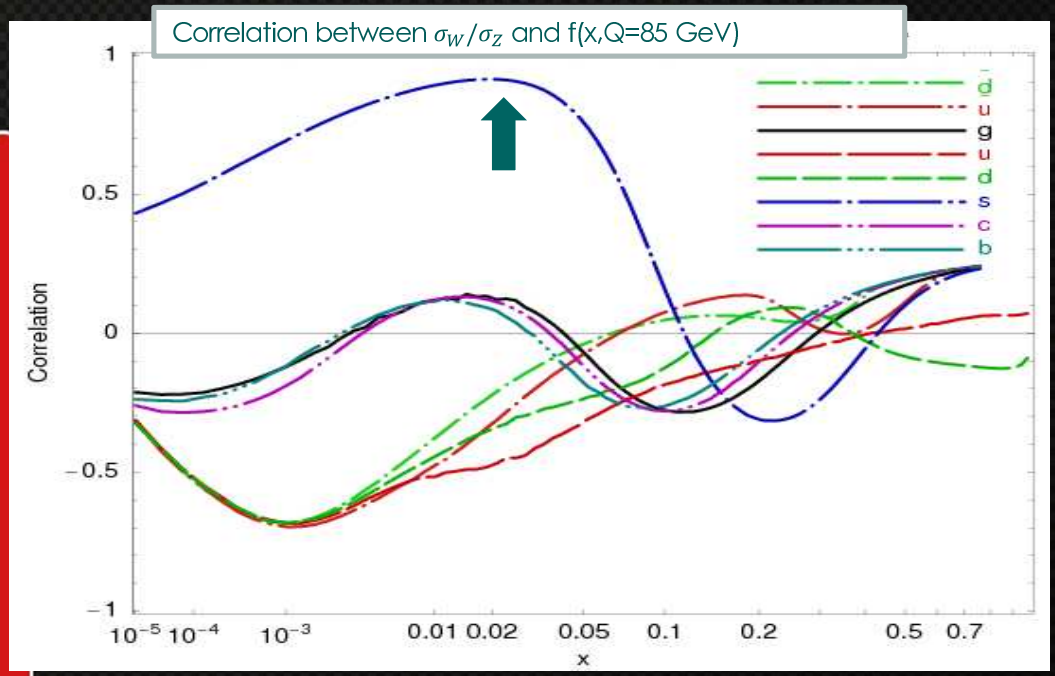

2008, CTEQ6.6 (arXiv:0802.0007): the ratio σ_W/σ_Z at LHC must be sensitive to the strange PDF $s(x,Q)$

The uncertainty on $s(x,Q)$ limits the accuracy of the W boson mass measurement at the LHC

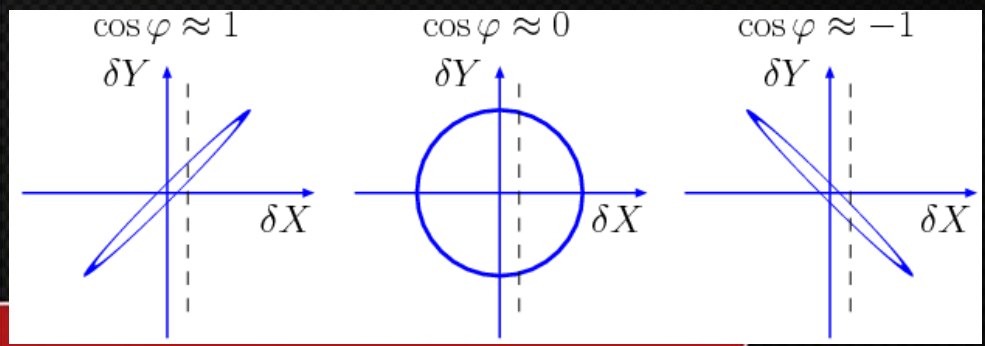

Correlation cosine $\cos\varphi \approx \pm 1$:

⇔ Measurement of X imposes tight constraints on Y

Constraining strangeness PDF by LHC W and Z cross sections

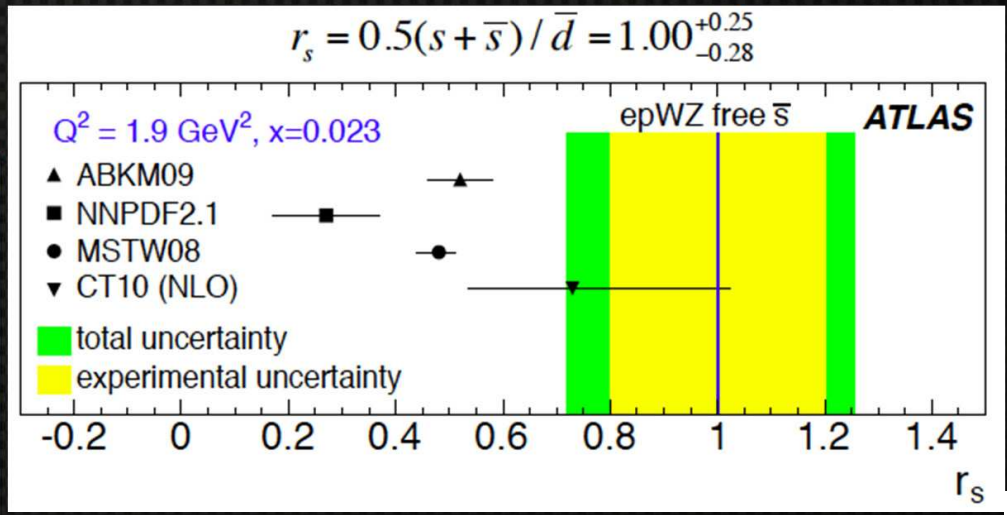

2012: the ATLAS analysis (arXiv:1203.4051) of W and Z production suggests

$\bar{s}(x,Q)/\bar{d}(x,Q) = 1.00^{+0.25}_{-0.28}$

at $x = 0.023$ and $Q^2 = 1.9$ GeV^2

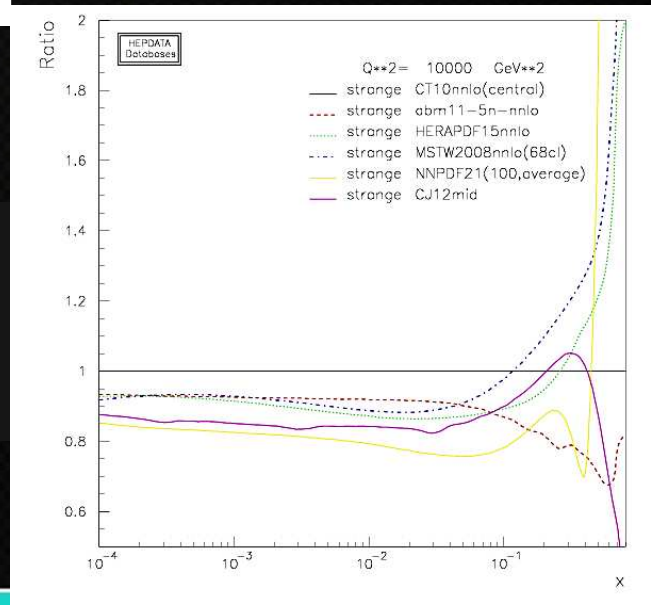

Similarly, $\sigma(W^+c)/\sigma(W^-c)$ cross section ratios show preference for $\frac{\bar{s}(x,Q)}{\bar{d}(x,Q)} \sim 1$, larger than in most pre-LHC PDF sets

f

$\alpha_s(M_Z)$ and heavy-quark masses in the PDF fits

- The QCD coupling, $\alpha_s(M_Z)$, and $\overline{MS}$ heavy-quark masses, $m_c(m_c)$, $m_b(m_b)$, and $m_t(m_t)$, can be also varied in the PDF fits.

  However, the resulting constraints on these parameters are much weaker than from their dedicated measurements.

- CT14 NNLO assumes a fixed $\alpha_s(M_Z) = 0.118 \pm 0.002$ at 90%c.l., which is equal to the world average $\alpha_s(M_Z)$.

  For any X, the α_s uncertainty $\Delta_{\alpha_s} X$ is correlated with the PDF uncertainty $\Delta_{PDF} X$, the two must be combined in the full prediction.

  CT10 provides PDF error sets to compute the PDF+α_s uncertainty with full correlation.

Constraints on $\alpha_s(M_Z)$ and the $\overline{MS}$ charm mass $m_c(m_c)$ in the CT10 NNLO fit

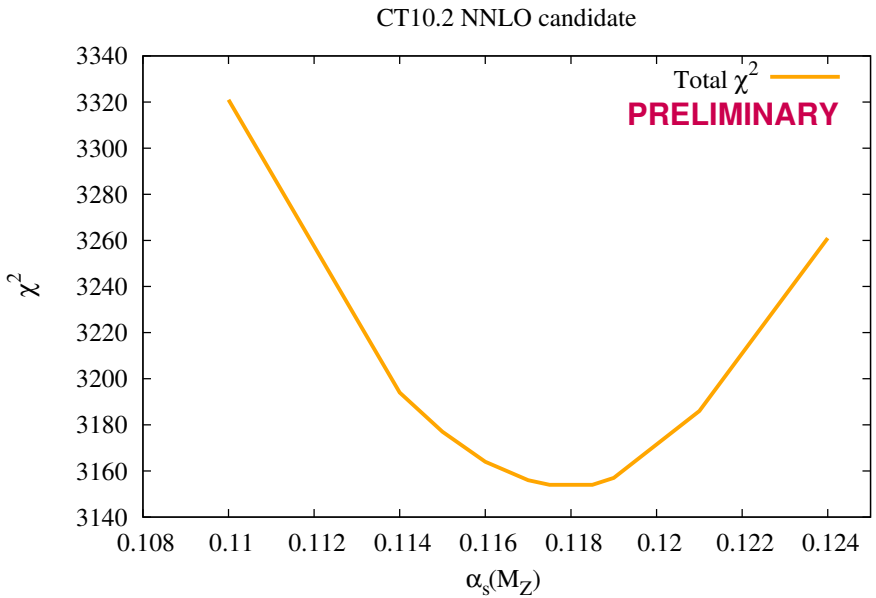

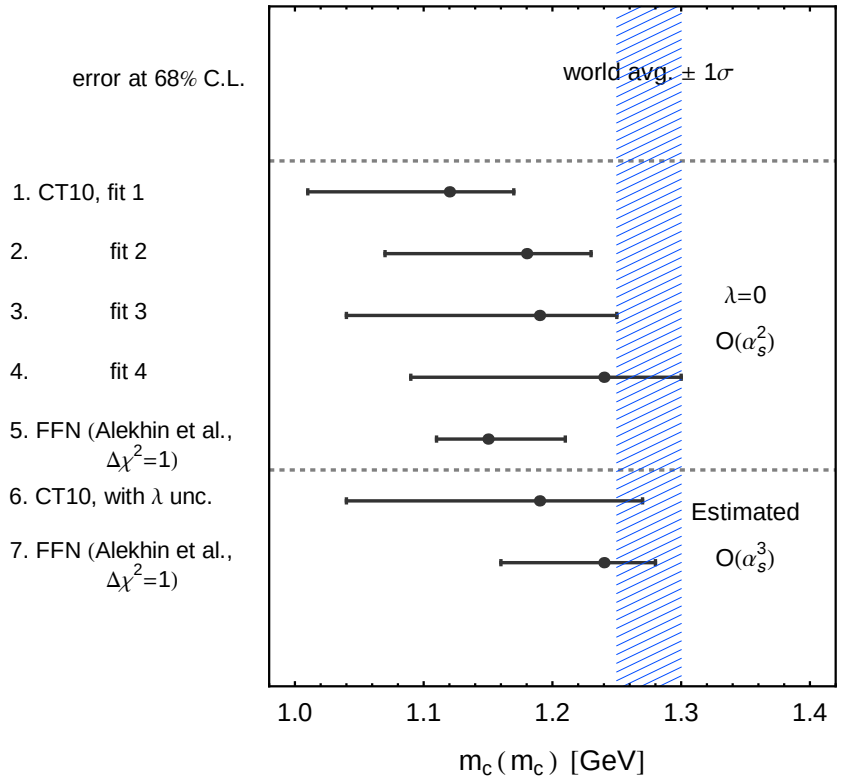

- NLO: $\alpha_s(M_Z) = 0.11964 \pm 0.0064$ at 90% c.l.
- NNLO: $\alpha_s(M_Z) = 0.118 \pm 0.005$

Gao, Guzzi, Nadolsky, 1304.0494
$m_c(m_c) = 1.19^{+0.08}_{-0.15}$ GeV at 68% c.l.

$\alpha_s(M_Z)$ and heavy-quark masses in the PDF fits

- The QCD coupling, $\alpha_s(M_Z)$, and $\overline{MS}$ heavy-quark masses, $m_c(m_c)$, $m_b(m_b)$, and $m_t(m_t)$, can be also varied in the PDF fits.

  However, the resulting constraints on these parameters are much weaker than from their dedicated measurements.

- CT14 NNLO assumes a fixed $\alpha_s(M_Z) = 0.118 \pm 0.002$ at 90%c.l., which is equal to the world average $\alpha_s(M_Z)$.

  For any X, the α_s uncertainty $\Delta_{\alpha_s} X$ is correlated with the PDF uncertainty $\Delta_{PDF} X$, the two must be combined in the full prediction.

  CT10 provides PDF error sets to compute the PDF+α_s uncertainty with full correlation.

CT10 estimate of the PDF+α_s uncertainty

CT10 NNLO set provides

- $2N+1=51$ PDF error sets at $\alpha_s(M_Z)=0.118$, to compute

$$\Delta_{PDF}X=\frac{1}{2}\sqrt{\sum_{i=1}^{25}\left(X_i^{(+)}-X_i^{(-)}\right)^2}$$ (the PDF uncertainty);

- 2 best-fit PDFs for for $\alpha_s=0.116$ and 0.120, to compute

$$\Delta_{\alpha_s}X=\frac{X(\alpha_s=0.120)-X(\alpha_s=0.116)}{2}$$ (the α_s uncertainty).

The formula for the combined PDF+α_s uncertainty with **with full correlation** is *(Lai et al., 1004.4624)*

$$\Delta_{PDF+\alpha_s}X=\sqrt{(\Delta_{PDF}X)^2+(\Delta_{\alpha_s}X)^2}$$

Combination of PDF uncertainties from several groups

As the final step, it may be necessary to combine QCD cross sections X_i from several PDF ensembles and find the ultimate PDF uncertainty. The 2015 PDF4LHC recommendation provides guidelines for combination and three PDF4LHC'15 PDF sets constructed from CT14, MMHT'14, and NNPDF3.0 PDF sets

The META PDF method first averages the input PDFs in the PDF parameter space, before computing X_i *(J. Gao, P. Nadolsky, 1401.0013).*